
A Dedicated Mechanism for DNA-Protein Crosslink Repair

DISSERTATION DER FAKULTÄT FÜR BIOLOGIE
DER LUDWIG-MAXIMILIANS-UNIVERSITÄT MÜNCHEN



vorgelegt von
Diplom-Biologe Julian Stinglele

17. Oktober 2014

EIDESSTATTLICHE ERKLÄRUNG

Hiermit erkläre ich an Eides statt, dass ich die vorliegende Dissertation selbstständig und ohne unerlaubte Hilfe angefertigt habe. Ich habe weder anderweitig versucht, eine Dissertation einzureichen oder eine Doktorprüfung durchzuführen, noch habe ich diese Dissertation oder Teile derselben einer anderen Prüfungskommission vorgelegt.

München, den.....

.....

(Unterschrift)

Promotionsgesuch eingereicht am: 14.10.2014

Datum der mündlichen Prüfung: 21.01.2015

Erster Gutachter: Prof. Dr. Stefan Jentsch

Zweiter Gutachter: Prof. Dr. Peter Becker

Die vorliegende Arbeit wurde zwischen April 2010 und September 2014 unter der Anleitung von Prof. Dr. Stefan Jentsch am Max-Planck-Institut für Biochemie in Martinsried durchgeführt.

Wesentliche Teile dieser Arbeit sind in folgenden Publikationen veröffentlicht und zusammengefasst:

Stingele, J., Schwarz, M.S., Bloemeke, N., Wolf, P.G. and Jentsch, S. (2014)

A DNA-dependent protease involved in DNA-protein crosslink repair.

Cell, 158:327-38.

Stingele, J., Habermann, B. and Jentsch, S.

DNA-protein crosslink repair: proteases as DNA repair enzymes.

Trends in Biochemical Sciences, commissioned review in preparation.

Summary.....	1
1 Introduction	2
1.1 Mechanisms of DNA repair	2
1.1.1 Excision repair.....	2
1.1.2 DNA double-strand break repair.....	6
1.1.3 Postreplicative repair.....	7
1.1.4 Inter-strand crosslink repair.....	8
1.2 DNA-protein crosslinks	10
1.2.1 Enzymatic DPCs	10
1.2.2 Nonenzymatic DPCs	11
1.2.3 Repair of DPCs	13
2 Aims of this study	15
3 Results	16
3.1 The metalloprotease Wss1 is involved in Top1cc repair.....	16
3.2 Wss1 interacts with the Cdc48 segregase and the SUMO system	20
3.2.1 Wss1 function requires direct interaction with Cdc48.....	20
3.2.2 Wss1 function is linked to the SUMO system.....	22
3.3 Wss1 is a DNA-dependent protease	24
3.4 Wss1 targets DNA-bound proteins.....	27
3.4.1 Wss1 is a DNA-binding protein	27
3.4.2 Wss1 cleaves DNA-binding proteins	28
3.5 Wss1 is involved in cellular resistance towards formaldehyde.....	31
3.6 Wss1-dependent DPC-processing directs repair pathway choice	36
4 Discussion	40
4.1 DNA-protein crosslink repair	40
4.1.1 DPC repair.....	40
4.1.2 DPC tolerance	42
4.2 Regulation of Wss1	43
4.2.1 Wss1 and SUMO.....	43
4.2.2 Wss1 and Cdc48.....	44
4.3 A conserved family of DPC proteases?.....	45
5 Materials and Methods	49
5.1 Microbiological techniques.....	49

5.1.1	<i>Escherichia coli</i> (<i>E. coli</i>) techniques	49
5.1.2	<i>Saccharomyces cerevisiae</i> (<i>S. cerevisiae</i>) techniques	52
5.2	Molecular biology techniques	61
5.2.1	General buffers and solutions	61
5.2.2	DNA purification and analysis	61
5.2.3	Polymerase chain reaction (PCR)	62
5.2.4	Molecular cloning	63
5.3	Biochemical techniques	63
5.3.1	Gel electrophoresis and immuno-blot techniques	64
5.3.2	Protein purification and interaction analysis	64
5.3.3	Protease assays.....	67
	References	69
	Abbreviations	78
	Acknowledgements	80
	Curriculum Vitae	81

Summary

DNA repair is pivotal for genome integrity to counteract the constant threat posed by DNA damage. DNA lesions if left unrepaired can cause genomic instability and ultimately cell death. DNA-protein crosslinks (DPCs) are particularly toxic lesions as they interfere with essential DNA transactions such as DNA replication or transcription. DPCs arise by ionizing irradiation and UV-light, are particularly caused by endogenously produced reactive compounds such as formaldehyde, and also occur during compromised topoisomerase action. Although nucleotide excision repair and homologous recombination contribute to cell survival upon DPCs, hardly anything is known about mechanisms that target the protein component of DPCs directly.

This study identifies the metalloprotease Wss1 as being crucial for cell survival upon exposure to formaldehyde and topoisomerase 1-dependent DNA damage. Yeast mutants lacking Wss1 accumulate DPCs and exhibit gross chromosomal rearrangements. Notably, *in vitro* assays indicate that substrates such as topoisomerase 1 are processed by the metalloprotease directly and in a DNA-dependent manner. Thus, this study suggests that Wss1 contributes to survival of DPC-harboring cells by acting on DPCs proteolytically. We propose that DPC proteolysis enables repair of these unique lesions via downstream canonical DNA repair pathways and thereby promotes replication completion in the face of DPCs.

1 Introduction

Ensuring that the genetic information is passed on faithfully to the next generation is integral to every form of life. This task, however, is challenged by constant assaults on the integrity of DNA. DNA lesions trigger mutagenesis and genome instability and thus contribute to tumorigenesis and aging (Hoeijmakers, 2001). As a consequence, DNA repair pathways have evolved that counteract these threats (Friedberg et al., 2014).

1.1 Mechanisms of DNA repair

DNA repair is defined as the cellular process, which restores the normal sequence and structure of damaged DNA (Friedberg et al., 2014). The importance of functional DNA repair is highlighted by the fact, that cancer cells frequently display mutations in DNA repair genes (Furgason and Bahassi el, 2013). DNA repair deficiency results in mutagenesis and genome instability, which enables cancer cells to acquire new functions such as the disruption of tumor suppressor genes and/or the activation of oncogenes (Jackson and Bartek, 2009). Notably, the abrogation of DNA repair mechanisms is also responsible for the strong sensitivity of cancer cells to DNA damage inducing agents, which is exploited for cancer treatment by irradiation or chemotherapy (Helleday et al., 2008; Zamble and Lippard, 1995). As DNA lesions are very diverse in nature, they require highly specific pathways for their repair (Friedberg et al., 2014). Owing to intensive research efforts the repair factors needed for most types of lesions are known and the underlying mechanisms are generally well understood (Friedberg et al., 2014).

1.1.1 Excision repair

Excision repair comprises mechanisms, which excise damaged DNA fragments are excised, followed by re-synthesis of the resulting gap. Excision repair includes the repair of single damaged DNA bases (base excision repair, BER), small nucleotide tracks (nucleotide excision repair, NER) as well as DNA mismatches (mismatch repair, MMR) (Figure 1). All excision mechanisms share a common order of events: recognition, incision, repair synthesis and finally ligation.

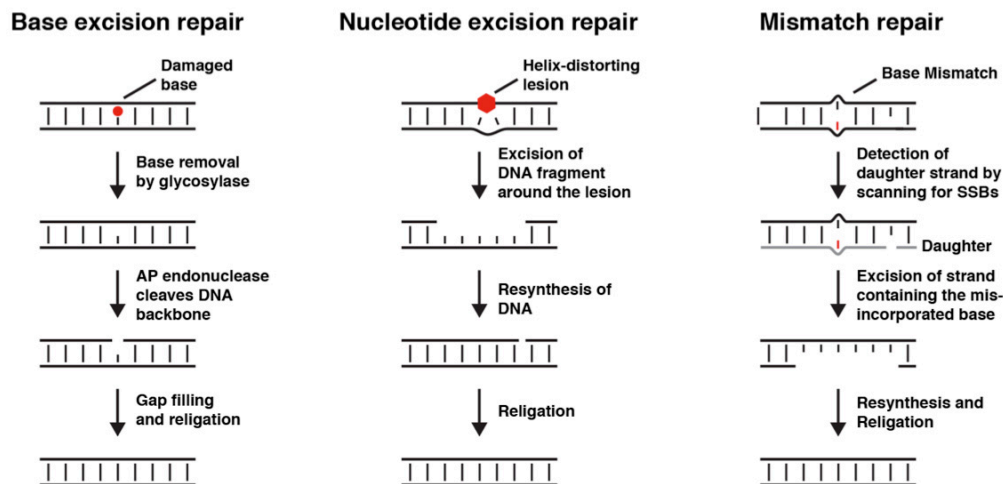


Figure 1: Principles of excision repair. Schematic depiction of the excision repair mechanisms base excision repair, nucleotide excision repair and mismatch repair. Figure based on illustrations in (D'Andrea, 2008).

Base excision repair

BER targets DNA bases damaged by oxidation, alkylation, deamination or hydrolysis. BER is initiated by binding of DNA-glycosylases to the damaged bases (Krokan and Bjørås, 2013). DNA-glycosylases (five in yeast, at least 11 in humans) are specific for certain types of base modifications (Memisoglu and Samson, 2000). 8-oxoguanine, for instance, is specifically targeted by the OGG1 glycosylase (Boiteux and Radicella, 2000). Upon binding, the damaged base is excised by the glycosylase resulting in an apurinic/aprimidinic (AP) site. The AP site is then cleaved by an AP-endonuclease followed by end processing by an AP-lyase. Together this results in a single nucleotide gap, which is then filled by insertion of a single nucleotide (short-patch BER) or between 2 - 10 nucleotides (long-patch BER) (Zharkov, 2008). The generally dominant short-patch BER employs the specialized DNA polymerase β for gap filling, with repair being completed through ligation by DNA ligase 1 or 3 (Sobol et al., 1996). In contrast, long patch repair uses the canonical replication machinery (DNA polymerases δ/ϵ , the replication clamp PCNA (proliferating cell nuclear antigen, pol30 in yeast), DNA Ligase 1 and FEN1 (Rad27 in yeast)) for gap filling and ligation and operates mainly in S-phase (Levin et al., 2000; Prasad et al., 2000; Stucki et al., 1998).

Nucleotide excision repair

NER uses a strategy distinct from the direct recognition employed by BER for identifying sites of DNA damage. Rather than being specific to certain adducts, NER

identifies lesions by recognizing distortions in the structure of DNA caused by the lesion (Nospikel, 2009). Lesions resulting in alterations of the DNA structure, and accordingly those repaired by NER, are mainly bulky adducts, such as those caused by UV-light (e.g. thymidine dimers) (Wood, 1999). Consequently, cells deficient for NER are explicitly sensitive toward UV-light exposure. Mutations in NER genes result in the genetic disorder xeroderma pigmentosum (XP), which is characterized by an extreme sensitivity to sunlight and a drastically increased risk for the development of skin cancer (de Boer and Hoeijmakers, 2000; DiGiovanna and Kraemer, 2012). NER can be initiated by two distinct mechanisms, global genome repair (GGR) and transcription coupled repair (TCR), which however subsequently merge into the same pathway (Schärer, 2013; Vermeulen and Fousteri, 2013).

GGR is initiated by binding of the heterodimer XPC-RAD23B (Rad4-Rad23 in *S. cerevisiae*) to the DNA strand opposing the lesion, which is thermodynamically destabilized by the presence of the lesion (Min and Pavletich, 2007). This explains the versatility of NER, as recognition is completely independent of the identity of the lesion itself. Alternatively, GGR can be initiated by the DDB complex, which is able to specifically recognize lesion that cause rather little distortions, such as cyclobutane pyrimidine dimers (Fei et al., 2011). After lesion recognition the DDB complex triggers recruitment of XPC-RAD23B. In both cases, GGR proceeds by XPC-RAD23B recruiting the multi-subunit complex TFIIH (Compe and Egly, 2012). TFIIH contains two helicases, XPB and XPD, which unwind the DNA around the lesion, resulting in a denaturation bubble of roughly 30 nucleotides (Schärer, 2013). At this stage, XPA is recruited to the complex and displaces the XPC complex. Next, the two endonucleases XPF and XPG join the repair assembly and incise the DNA in 5', respectively 3', of the lesion (Fagbemi et al., 2011). After excision of the damaged DNA, the 3' hydroxyl group generated during cleavage by XPF is used for initiation of repair synthesis to fill the DNA gap (Ogi et al., 2010). Finally, ligation by LIG 1 or 3 completes the NER reaction. The final steps of repair (incision, gap filling and ligation) are identical for TCR, however the lesion is recognized by stalling of RNA polymerase II (RNAPII) at damaged sites within the transcribed strand (Vermeulen and Fousteri, 2013). Stalled RNAPII initiates TCR by attracting NER enzymes, resulting in the formation of the aforementioned denaturation bubble. This bypasses the need for XPC, but requires additional TCR specific factors (e.g. CSA and CSB). Notably, the unscheduled DNA synthesis (i.e. outside of S-phase) during gap filling, is a hallmark of NER and is not only used as an experimental tool to monitor NER

activity, but also during diagnosis of XP (DiGiovanna and Kraemer, 2012). In fact, the finding that cells from XP patients are deficient for UV-induced unscheduled DNA synthesis, established the connection between NER and XP (Cleaver, 1968).

Mismatch repair

MMR does not target DNA damage in the sense of chemical or physical alterations, but is able to recognize and repair mispaired nucleotides (Jiricny, 2013). Mismatches, defined as non Watson-Crick base pairs, occur mostly during replication by incorporation of wrong nucleotides by DNA polymerases (Arana and Kunkel, 2010). Notably, there is only a short window for repair, as the mismatch will be converted to a mutation during the next round of replication and will therefore no longer be recognizable. Consequently, cells deficient for MMR display very high mutagenesis rates and mutations of MMR genes are causative for cancer predisposition in patients with Lynch syndrome (also known as hereditary nonpolyposis colon cancer, HNPCC) (Lynch et al., 2009). A unique challenge during MMR is the identification of the strand containing the correct nucleotide. This is achieved by the ability of MMR to distinguish between the parental and the newly synthesized daughter strand, which contains the wrong nucleotide. Recognition of the daughter strand is linked to the fact, that MMR requires strand discontinuities for initiation of repair. Nicks are frequently present in the lagging strand, explaining why MMR is more efficient on the lagging strand (Pavlov et al., 2003). In addition, nicks can be *de novo* generated either by the endonuclease activity of the MutL α complex or by RNaseH2, which generates nicks within the daughter strand at ribonucleotides misincorporated during replication (Ghodgaonkar et al., 2013; Jiricny, 2013). After binding to the mismatch, MMR scans the surrounding DNA for these nicks. Initiating from the nick, the exonuclease EXO1 (Exo1 in yeast) starts to degrade the strand containing the misincorporated nucleotide (Tishkoff et al., 1998). Finally, the canonical replicative machinery fills the gap and incorporates the correct base at the site of the former mismatch.

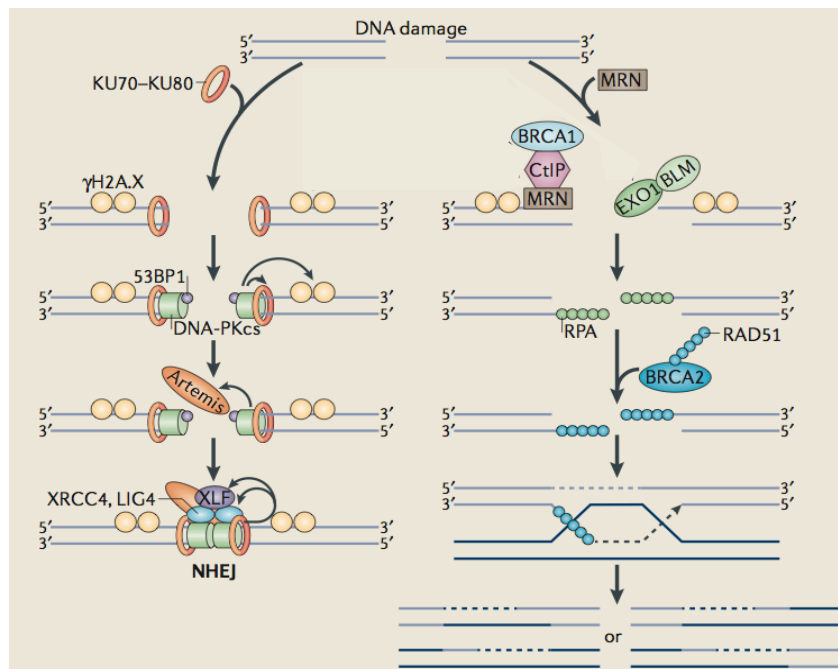


Figure 2: Cellular mechanisms for the repair of DNA double-strand breaks: Non-homologous end joining (left) and homologous recombination (right). See main text for details; Figure adapted from (Chowdhury et al., 2013).

1.1.2 DNA double-strand break repair

DNA double-strand breaks (DSB) are very toxic lesions, as a failure to repair a DSB results in the loss of genetic information, genomic rearrangements and potentially cell death (Khanna and Jackson, 2001). Notably, DSBs are not only induced by exogenous agents such as ionizing radiation (IR), reactive oxygen species or certain antineoplastic drugs (e.g. bleomycin), but are also generated physiologically during meiosis or immunoglobulin class switching (Mehta and Haber, 2014). Two major pathways exist for repairing DSBs, homologous recombination (HR) and non-homologous end joining (NHEJ) (Chapman et al., 2012) (Figure 2).

Homologous recombination

HR provides highly accurate repair of DSBs, as it uses an intact homologous DNA sequence as a template. Accordingly, HR is dependent on the presence of a homologous template, which will be in most cases the sister chromatid. As a sister chromatid is only available in the S- or G2-phase of the cell cycle, HR is restricted to these cell cycle phases. HR is initiated by rapid binding of the MRN (MRE11, RAD50, NBS1) complex (MRX (Mre11, Rad50, Xrs2) in yeast) to the break site (Heyer et al., 2010). MRN collaborates with CtIP (Sae2 in yeast) to produce short 3'-single-stranded DNA overhangs via its nuclease activity (Symington, 2014). These overhangs, which are readily covered by the single-strand binding protein RPA, can

be further extended by long-range resection mediated either by the exonuclease EXO1 (Exo1 in yeast) or the BLM helicase (Sgs1 in yeast) (Ferretti et al., 2013). Next, the recombinase RAD51 (Rad51 in yeast) is loaded on the single-stranded DNA, thereby replacing RPA, in a reaction mediated by BRCA2 (Rad52 in yeast) (Heyer et al., 2010). The resulting Rad51 filament is now able to probe the genome for homologous sequences (Renkawitz et al., 2014; Renkawitz et al., 2013). After identification of a homologous sequence, the RAD51 filament-mediated strand invasion enables extension of the 3'-end of the DSB with the homologous sequence as a template. Following end extension, the double Holliday junction formed during repair needs to be removed. This is achieved either by the action of resolvases (GEN1 (Yen1 in yeast) or MUS81-EME1 (Mus81-Mms4 in yeast)) or by dissolution mediated by the BTR (STR in yeast) complex (Sarbjana and West, 2014).

Non-homologous end joining

In contrast to HR, NHEJ operates mainly during the G1-phase of the cell cycle and employs a rather pragmatic repair principle. Instead of restoring the original sequence NHEJ simply “glues” the two ends of the DSB back together, which is frequently accompanied by deletions or insertions (Chiruvella et al., 2013; Lieber, 2010). NHEJ is initiated by recognition of the DSB ends by heterodimeric complex Ku (Ku70 and Ku80). The toroidal Ku complex bound to the DNA end acts as a node organizing the downstream events of NHEJ (Lieber, 2010). Ku promotes binding of the DNA-dependent kinase DNA-PKcs to the DSB end, which in turn activates the serine/threonine kinase activity of DNA-PKcs (Hartley et al., 1995; West et al., 1998). DNA-PKcs dependent phosphorylation stimulates end-processing by the Artemis nuclease (Goodarzi et al., 2006). The processed ends are subsequently ligated by LIG4, XRCC4 and XLF to complete repair.

1.1.3 Postreplicative repair

Postreplicative repair (PRR) is strictly speaking a DNA damage tolerance mechanism rather than a DNA repair mechanism, as PRR enables replication and thus survival in the face of DNA lesions without actually repairing them. If the replicative DNA polymerase encounters a DNA lesion (e.g. an alkylated base) it is likely to stall, as its active site is very narrow and it is therefore unable to accommodate damaged bases. The replicative helicase, however, will proceed unwinding the DNA duplex, thus resulting in an uncoupling of DNA unwinding and DNA synthesis (Blastyák, 2014). Uncoupling leads to the formation of single-stranded DNA, whose accumulation

triggers the PRR pathway by recruiting the ubiquitin E3 ligases Rad18 and Rad5 (Moldovan et al., 2007). Together with the E2 conjugation enzyme Rad6, Rad18 mono-ubiquitylates the replication clamp PCNA resulting in the activation of the error-prone branch of PRR (Hoege et al., 2002). In addition, mono-ubiquitylated PCNA can be further modified by Rad5, together with the E2 Ubc13/Mms2, resulting in the formation of a K63-linked ubiquitin chain, which triggers the error free branch of PRR (Hoege et al., 2002). Mono-ubiquitylated PCNA is recognized by specialized translesion synthesis (TLS) polymerases, which have a more promiscuous active site and are thus able to incorporate nucleotides opposite to the lesion (Bienko et al., 2005). TLS polymerases, however, insert wrong nucleotides frequently, thus resulting in the induction of mutagenesis. In contrast, the error-free branch of PRR allows replication of the damaged template by using the sequence information of the newly synthesized sister chromatid (Branzei, 2011). Despite the fact that several factors required for this reaction, termed template switching, are known, the precise mechanism remains enigmatic.

1.1.4 Inter-strand crosslink repair

Inter-strand crosslinks (ICLs) are very unique lesions, as they require not only a single pathway for repair, but carefully orchestrated sequential repair events, contributed by several canonical repair pathways (Moldovan and D'Andrea, 2009). ICLs arise by chemical crosslinking of the two strands of the DNA-double helix (Noll et al., 2006). They are particularly toxic as they inhibit strand separation during replication and thus block approaching replication forks (Vare et al., 2012). Consequently, rapidly dividing cells, such as malignantly transformed cancer cells, are especially sensitive to ICLs. Therefore, ICL-inducing agents (e.g. cisplatin derivatives or mitomycin C) are frequently used in anti-cancer therapy (Deans and West, 2011).

The current model for ICL repair, the dual fork convergence model, implies that repair is initiated when two replication forks stall on both sides of the crosslink (Raschle et al., 2008; Zhang and Walter, 2014). Next, the replicative helicases are evicted in a process mediated by BRCA1 (Long et al., 2014), followed by endonucleolytic incisions on either side of the ICL. The identity of the endonucleases responsible for incision is, however, under debate (Zhang and Walter, 2014). The “unhooked” ICL is now bypassed in a two-step process. First, TLS polymerases synthesize over the lesion. Second, the DSB generated during incision is repaired by

homologous recombination using the sister chromatid, which was already repaired during the TLS step, as a template (Long et al., 2011).

Fanconi anemia pathway

The different repair activities required for ICL repair are coordinated by the Fanconi anemia pathway (Moldovan and D'Andrea, 2009). Mutations in genes coding for Fanconi anemia proteins (FANCs) result in the rare genetic disorder Fanconi anemia, which is characterized by bone marrow failure and cancer predisposition (D'Andrea, 2010). Notably, Fanconi anemia patient cells are extremely sensitive toward crosslinking agents. In fact, cellular sensitivity to crosslinking agents is used as a diagnostic measure.

FANC proteins can be separated in three groups. The eight “group I” proteins are members of a large multi-subunit E3 ligase, which mediates mono-ubiquitylation of the two “group II” proteins FANCD2 and FANCI (the ID complex). The remaining “group II” FANC proteins are members of the repair pathways mentioned above required for ICL repair. For example, homozygous mutations in the gene encoding BRCA2, which is essential for the recombination step of ICL repair, result in Fanconi anemia (D'Andrea, 2010). The DNA damaged induced mono-ubiquitylation of the ID complex is critical for its localization on chromatin (de Oca et al., 2005). At the ICL the ID complex is crucial for stimulating the incision step during ICL repair (Knipscheer et al., 2009), thus explaining the sensitivity of Fanconi anemia patient cells to ICLs.

1.2 DNA-protein crosslinks

Unique DNA lesions are DNA-protein crosslinks (DPCs), which are defined as proteins covalently linked to DNA. DPCs are caused by permanent trapping of normally transient covalent enzyme-DNA reaction intermediates (enzymatic DPCs) and by chemical reactions caused by a variety of exogenous and endogenous agents (non-enzymatic DPCs) (Figure 3).

1.2.1 Enzymatic DPCs

The organization of the extremely large DNA molecules within the confined space of a nucleus poses a challenge to all eukaryotic cells. All processes involving DNA, such as replication or transcription, result in the formation of positive or negative supercoiling. To control these topological changes cells employ several enzymes called topoisomerases. For instance, topoisomerase 1 (Top1) relaxes torsional stress within a DNA molecule by cleaving one strand of the DNA duplex. The generated single-strand break (SSB) allows rotation of the DNA strand, thereby relieving the supercoils within the DNA (Champoux, 2001). The enzyme remains covalently linked to the 3'-end of the SSB during this reaction. This covalent complex is referred to as Top1cc (Top1 cleavage complex). Normally, the relaxation reaction is completed by Top1 resealing the SSB. However, this can be inhibited by nearby DNA damage, such as abasic sites, which result in a distortion of the DNA (Pourquier et al., 1997). The distortion prohibits proper alignment of the free 5'-end of the SSB, thus rendering

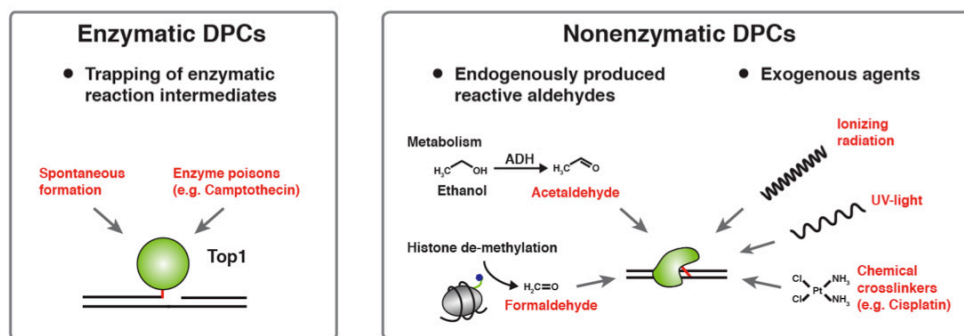


Figure 3: Sources of DPCs. Enzymatic DPCs are caused by trapping of normally transient covalent enzyme-DNA reaction intermediates. Topoisomerase 1 (Top1) can be trapped if nearby DNA damage (such as abasic sites) inhibits completion of the enzymatic reaction cycle. Top1-trapping can also be induced by small molecules, such as camptothecin, which intercalates within the enzyme-DNA interface. Nonenzymatic DPCs are caused by unspecific chemical crosslinking of proteins to DNA by agents originating from endogenous and exogenous sources. Reactive aldehydes, e.g. acetaldehyde and formaldehyde are produced metabolically from ethanol oxidation or histone de-methylation, respectively. Exogenous agents causing DPCs include IR, UV-light and chemical crosslinkers, such as platinum-based anticancer drugs (e.g. cisplatin).

it impossible for Top1 to religate the two ends. Consequently, Top1 remains covalently linked to the DNA. Top1ccs are not only trapped due to nearby DNA damage, but also by the alkaloid camptothecin (CPT). CPT intercalates within the Top1cc, thus inhibiting religation (Pommier, 2006). Top1ccs are very dangerous lesions, as during replication an approaching fork may convert the SSB into a DSB. Thus Top1ccs are especially toxic in rapidly dividing cells, which is exploited during anti-cancer therapy with camptothecin analogs such as topotecan.

Similarly, topoisomerase 2 (Top2) can be trapped on DNA as a covalent complex. Top2 differs from Top1, as it introduces not only a SSB but a DSB. A second DNA molecule is traversed through the DSB prior to religation of the DSB. This allows Top2 not only to remove, but also to introduce supercoiling. Analogous to inhibition of Top1 by CPT, Top2 can be trapped by the anti-cancer drug etoposide. Etoposide interferes with the Top2 enzymatic reaction after introduction of the DSB, thus potentially inducing DSBs. Interestingly, the ability of Top2-like enzymes to generate DSBs is also utilized intentionally by cells to introduce breaks during meiosis. The Top2-like topoisomerase Spo11 introduces DSBs during meiosis, thus allowing meiotic recombination. After cleaving the DNA duplex one Spo11 molecule remains attached to each end of the DSBs, which needs to be removed to allow recombination.

1.2.2 Nonenzymatic DPCs

Nonenzymatic DPCs are distinct from enzymatic DPCs, as the crosslinked protein might be any protein in the vicinity of DNA, in contrast to enzymatic DPCs, which involve only specific proteins. Crosslinking is caused by reactive molecules, which react on the one hand with the DNA and on the other with a protein (Barker et al., 2005). As a result, a covalent bond between DNA and protein is formed. The agents responsible for crosslinking can be classified by their origin, which can be either exogenous or endogenous.

Exogenous sources

IR produces locally high levels of reactive oxygen species, which then trigger various types of chemical reactions resulting in several types of DNA lesion (Ravanat et al., 2014). This includes SSBs, DSBs (as a result of two SSBs in close proximity), base damage and DPCs. Most research activities in the past focused on IR-induced DSBs, however similar amounts of DSBs and DPCs are formed by exposure to IR (Barker et al., 2005). Interestingly, there is a direct connection between the ratio of DSBs and

DPCs induced by IR. Irradiation in the presence of oxygen mostly produces DSBs, whereas IR exposure under hypoxic conditions (i.e. in the absence of oxygen) results almost exclusively in the formation of DPCs (Meyn et al., 1987; Zhang et al., 1995). DPCs are also induced by UV light (Chodosh, 2001). However, the exact mechanism by which this occurs is not entirely clear. Probably, two mechanisms are involved, a direct mechanisms as well as crosslinking mediated by UV-induced ROS (Peak et al., 1985). Generally, any agent resulting in the production of ROS leads to the formation of DPCs. This is also the case for reactive nitrogen species, such as nitric oxide (NO), which are, for instance, produced by immune cells in order to kill invading pathogens. DNA exposure to NO results in the formation of oxanine, a damaged base derived from guanine (Nakano et al., 2003). Oxanine is highly reactive towards the amino groups of lysine and arginine and thus potently induces DPCs (Chen et al., 2007a; Nakano et al., 2003). In addition, most of the aforementioned ICL-inducing anti-neoplastic drugs (cisplatin-derivatives, mitomycin C) also produce DPCs, which might also contribute to their therapeutic efficacy (Chvalova et al., 2007; Hincks and Coulombe, 1989). In addition, DPCs are caused by various environmental reactive substances, such as diepoxybutane (DEB), which is present in tobacco smoke (Gherezghiher et al., 2013).

Endogenous sources

Notably, various reactive compounds capable of crosslinking proteins to DNA are produced endogenously as metabolic intermediates. For instance, ethanol oxidation by alcohol dehydrogenase (ADH) generates the highly reactive acetaldehyde molecule. The toxicity of endogenously produced acetaldehyde was strikingly demonstrated by the finding that mice deficient for the acetaldehyde detoxifying enzyme ALDH2 develop leukemia and anemia if lacking functional DNA repair pathways in addition (Garaycochea et al., 2012; Langevin et al., 2011). Reactive aldehydes are even produced directly at chromatin, where every histone demethylation reaction produces one formaldehyde (FA) molecule (Kooistra and Helin, 2012). FA is extremely potent in crosslinking proteins to DNA, a feature commonly exploited for isolating DNA-protein complexes during chromatin immuno-precipitation (ChIP) experiments. Crosslinking occurs by FA reacting with free amino or imino groups of amino acid side chains or DNA bases to form a Schiff base, which then reacts with a second amino group (Lu et al., 2010; Ma and Harris, 1988). Notably, FA is classified as a carcinogen, as FA exposure results in nasopharyngeal cancer and squamous cell carcinomas in mammals (Swenberg et al., 2011). Similar to the

already mentioned ALDH2, the formaldehyde-detoxifying enzyme ADH5 is essential in cells lacking functional DNA repair pathways (Rosado et al., 2011).

1.2.3 Repair of DPCs

Despite the challenge DPCs pose for cellular integrity surprisingly little is known about how cells exactly respond to these insults. Some canonical DNA repair pathways are known to provide resistance towards DPC-inducing agents, but mechanistic insights are scarce. The only well-studied exception is the cellular response to topoisomerase-dependent DNA crosslinks, for which specific pathways are known and thought to be well understood (Pommier et al., 2006). Repair of Top1ccs is initiated by proteasomal degradation of Top1 (Desai et al., 1997). The remaining peptide attached to the DNA is subsequently removed by the action of tyrosyl-DNA phosphodiesterase 1 (Tdp1), which catalyzes the hydrolysis of the bond between Top1's tyrosine and the DNA's 3'-end (Pouliot et al., 1999). As discussed above, Top1ccs are especially toxic, as replication will convert the crosslink into a DSB. Consequently, mutants deficient in the HR pathway are extremely sensitive toward CPT-induced Top1ccs (Malik and Nitiss, 2004). In addition, endonucleases of

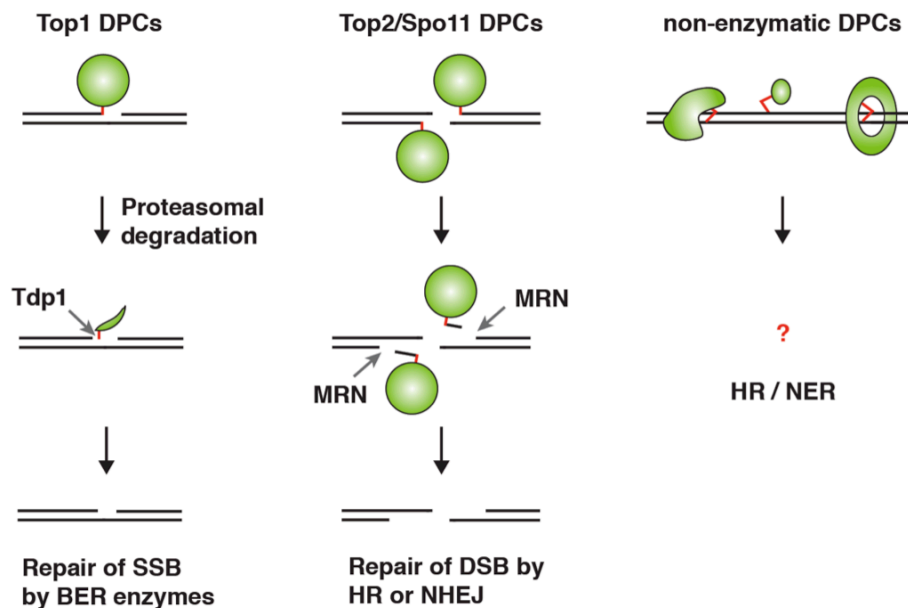


Figure 4: Depiction of different types of DPCs and cellular measures to repair them. Left panel: Top1-dependent DPCs are thought to be initially processed by proteasomal degradation. This enables access of the enzyme Tdp1, which hydrolyses the covalent bond between Top1's catalytic tyrosine residue and the 3'-end of the DNA. Middle panel: Top2 and Spo11 crosslinks are unique, as they involve a DSB. The MRN (MRX in yeast) nuclease is able to remove these lesions by merely cleaving of the protein moiety. Top2 adducts can be additionally removed by the enzyme Tdp2 (not shown). Right panel: The mechanistic details regarding the repair of nonenzymatic DPCs are currently elusive. However, it is known that both HR and NER contribute, as yeast mutants lacking either pathway are sensitive towards FA.

the NER pathway have been shown to provide resistance toward CPT, however their precise function in the repair of Top1ccs remains unclear (Vance and Wilson, 2002). Top2- and Spo11-dependent crosslinks are intrinsically distinct challenges, as the DPCs reside in these cases at the end of a DSB. Those DPCs are removed by the nuclease activity of the MRN (MRX in yeast) complex or by tyrosyl-DNA phosphodiesterase 2 (Tdp2) (Cortes Ledesma et al., 2009; Hartsuiker et al., 2009).

Nonenzymatic DPCs are very different from enzymatic with respect to the fact that almost any DNA-associated protein might be involved. Consequently nonenzymatic DPCs are expected to be very diverse in nature. Thus highly specialized enzymes like Tdp1, which almost uniquely targets Top1ccs, are impractical for their repair. It is known that general DNA repair pathways like HR and NER provide resistance towards FA-induced DPCs (de Graaf et al., 2009). However no general DPC repair pathway targeting specifically the protein components of DPCs, irrespective of its identity, has been described so far.

2 Aims of this study

Specific DNA repair and DNA damage tolerance pathways have been identified and characterized in depth for many types of DNA lesions. However, the potential threat caused by DNA-protein crosslinks has been rather neglected. DPCs are particularly toxic as they interfere with essential DNA transactions, such as DNA replication or transcription. Although nucleotide excision repair and homologous recombination have been implicated in DPC repair, no general DPC-specific pathway has been identified so far. Preliminary results from the Jentsch laboratory suggested a potential involvement of the poorly characterized metalloprotease Wss1 in the cellular response towards a special class of DPCs, namely Top1 cleavage complexes (Top1ccs). Genetic results indicated that Wss1 acts in a pathway parallel to the well-known repair factor Tdp1. However, the precise mechanistic contribution of Wss1 remained unclear.

This study aimed to identify the precise function of Wss1 in the cellular response to Top1ccs. Thus, the initial objective of this study was to clarify, if Wss1 acts directly on Top1ccs. If acting directly on Top1ccs, mutant cells lacking the enzyme should accumulate covalently trapped Top1. To address this question we initially aimed to establish an assay to visualize Top1ccs. In case evidence for a direct role of Wss1 in Top1cc repair could be obtained a second major aim of this study was to test by *in vitro* experiments if Wss1 might act directly and proteolytically on Top1.

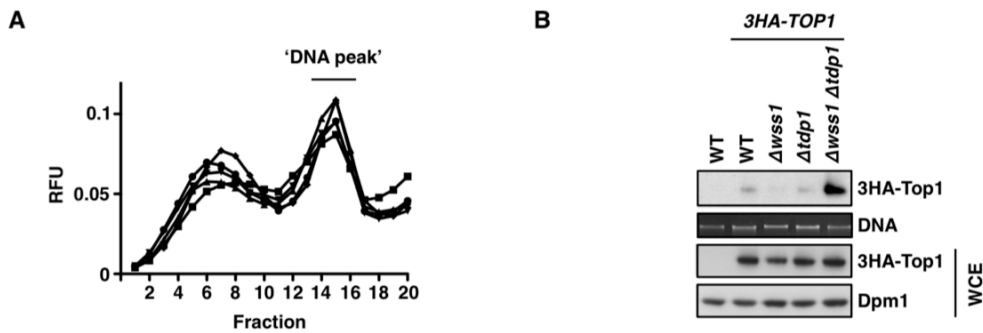


Figure 6. Top1ccs accumulate in cells lacking Wss1 and Tdp1. (A) Extracts of 3HA-Top1 expressing cells prepared under harsh denaturing conditions were subjected to cesium chloride gradient ultra-centrifugation. Gradients were fractionated using a liquid handling work station and DNA-containing fractions (typically found in the bottom fractions) were identified by staining with SYBR gold nucleic acid stain. DNA-containing fractions were pooled, concentrated and subjected to buffer exchange. (B) Purified DNA was then quantified using agarose gel electrophoresis, followed by ethidium bromide staining. Levels of 3HA-Top1 within the DNA fraction were determined by immuno-blotting with HA-specific antibodies after digestion of DNA with micrococcal nuclease. Top1 levels in whole cell extracts (prepared using the TCA method) are shown for comparison.

function in repairing Top1ccs is well known, it was tested if the slow growth of $\Delta wss1 \Delta tdp1$ mutant cells is related to the action of Top1. Astonishingly, it was found that deletion of the gene encoding Top1 rescued the sickness of $\Delta wss1 \Delta tdp1$ mutant cells almost entirely (PhD thesis M. Schwarz). These results were confirmed independently by spot dilution assays as well as tetrad dissection (Figure 5A-B). Additionally, it was suggested that the proteolytic activity of Wss1 is required for its function. This was inferred from the fact that a replacement of one of the histidines coordinating the Zn^{2+} ion within the catalytic center of Wss1 by alanine (H115A) abrogated its function (PhD thesis M. Schwarz). Interpretation of this mutant is, however, complicated by the fact that this amino acid replacement likely results in general structural alterations. To confirm the requirement of Wss1's proteolytic activity for its function a different active site variant was generated ($wss1^{EQ}$), with a replacement of the active site glutamate E116 by glutamine (not expected to result in general structural alterations, M. Groll, personal communication). This variant did not complement the growth defect of $\Delta wss1 \Delta tdp1$ cells, but the protein is slightly lower expressed than the WT protein (Figure 5C-D). To exclude that the failure to complement is solely due to lower expression levels, we overexpressed $wss1^{EQ}$ under control of the *ADH* promoter, which failed to complement as well, confirming that Wss1's catalytic activity is indeed essential in cells lacking Tdp1 (Figure 5C-D). Nevertheless, it remained unclear whether Wss1 would act directly on Top1ccs. We

reasoned that if acting directly on Top1ccs, the sickness of the $\Delta wss1 \Delta tdp1$ double mutant should be accompanied by high levels of Top1ccs. In order to visualize Top1ccs in yeast cells we developed an ICE (*in vivo* complex of enzyme) assay based on protocols used for Top1cc quantification in mammalian and *S. pombe* cells (Hartsuiker et al., 2009; Subramanian et al., 2001). In brief (see Materials and Methods for details), exponentially grown yeast cells were lysed under harsh denaturing conditions by bead beating. The lysate was then subjected to cesium chloride gradient ultracentrifugation, thereby separating proteins (remaining on top of the gradient) from DNA (typically found in the bottom fractions) (Figure 6A). As only proteins covalently linked to DNA are expected to migrate together with the DNA, the amount of Top1 in the DNA-containing fractions corresponds directly to the number of Top1ccs. Indeed, cells lacking both Wss1 and Tdp1 show high levels of Top1ccs (Figure 6B), indicating that Wss1 acts directly on Top1ccs in a pathway parallel to Tdp1.

Given the fact that Top1ccs are known to stall replication forks (Regairaz et al., 2011), we asked next if the high amounts of Top1ccs in $\Delta wss1 \Delta tdp1$ cells result in cell cycle defects. Indeed $\Delta wss1 \Delta tdp1$ cells strongly accumulate with a G2-like DNA content, which is not seen in single mutants, as judged by cell cycle analysis using flow cytometry. Importantly, this defect is completely dependent on the presence of Top1, as it is not manifested in cells lacking the gene coding for Top1 in addition (Figure 7A). Stalled replication forks are known to activate the DNA damage checkpoint (a signaling cascade orchestrating the cellular response to DNA damage).

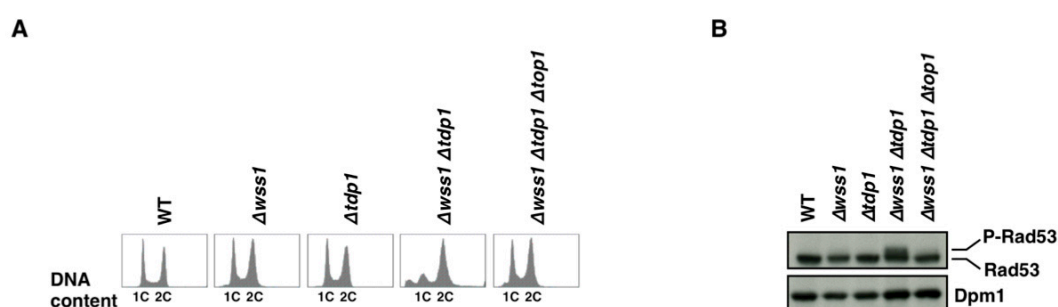


Figure 7. Cells lacking Wss1 and Tdp1 display Top1-dependent cell cycle defects and permanent DNA damage checkpoint activation. (A) Cells were collected from exponentially grown cultures, fixed, subjected to RNase and Proteinase digestion and finally stained with SYTOX green. Cell cycle profiles were recorded by flow cytometry. **(B)** Assessment of DNA damage checkpoint activation, as judged by phosphorylation of the checkpoint kinase Rad53. Cell extracts of exponentially grown cells were prepared by the TCA method and subjected to immuno-blotting using Rad53-specific antibodies. Dpm1 levels serve as loading control.

Consistently, we detected a permanent activation of the checkpoint, as judged by Rad53 phosphorylation. As observed for the growth defect and cell cycle arrest, the checkpoint activation was entirely dependent on the presence of Top1 (Figure 7B). Taken together we conclude that Wss1 and Tdp1 are part of two distinct pathways, which operate in parallel to counteract the threats posed by Top1ccs.

3.2 Wss1 interacts with the Cdc48 segregase and the SUMO system

3.2.1 Wss1 function requires direct interaction with Cdc48

During the initial characterization of Wss1 in the Jentsch laboratory several protein-protein interaction motifs were discovered in the C-terminal tail of Wss1 (PhD thesis M. Schwarz). Two short motifs resembling canonical sequences known to bind the

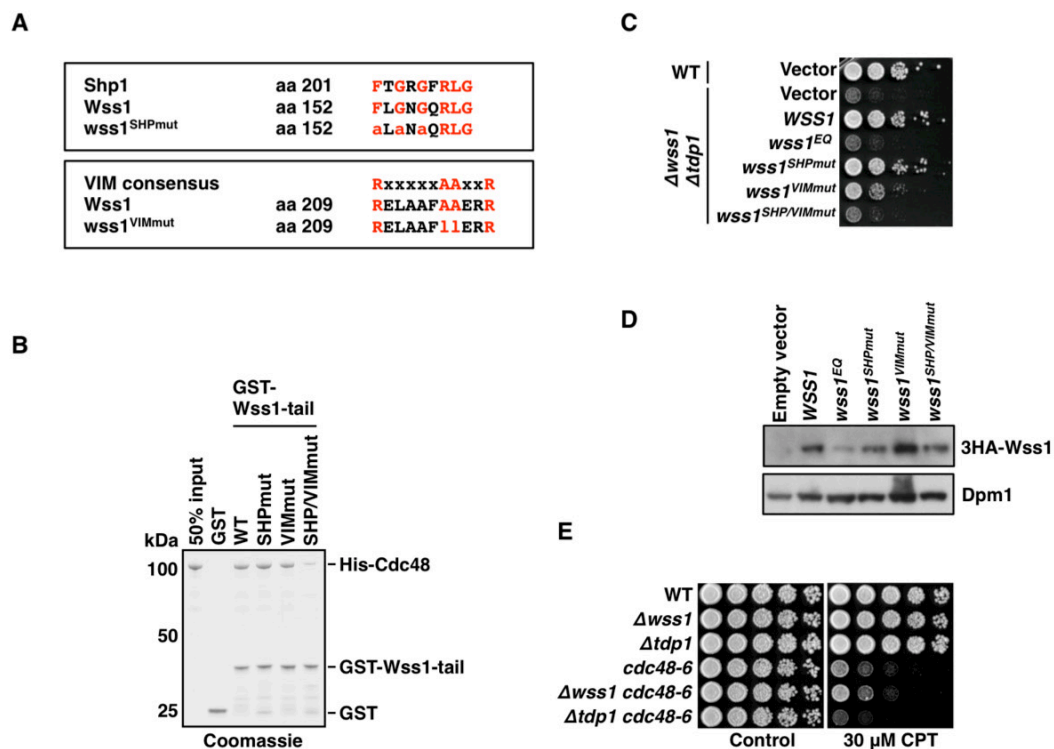


Figure 8. Interaction with Cdc48 is essential for Wss1's function. (A) Upper panel: Sequence of the SHP-box Cdc48 interaction motif within Wss1 is presented together with the sequence of the canonical Cdc48 interactor Shp1 for comparison. The amino acid replacements in the wss1^{SHPmut} variant are indicated as well. Lower panel: Sequence of the VIM consensus sequence is shown together with the sequence of the VIM found in Wss1. In addition the position and identity of amino acid replacements in the wss1^{VIMmut} variant are depicted. **(B)** Interaction of GST-tagged Wss1 fragments (aa148 - C-terminus) with His-tagged Cdc48 was tested by GST pull-down assays. GST-tagged Wss1-fragments as well as GST alone were coupled to GSH-Sepharose and incubated together with His-tagged Cdc48. Samples were incubated for 1 hr at 4°C prior to several wash steps and analysis by SDS-PAGE and Coomassie-blue staining. **(C)** Complementation of $\Delta wss1 \Delta tdp1$ cells with 3HA-tagged Wss1 variants with altered Cdc48 interaction motifs. Five-fold serial dilutions of cultures grown over night (adjusted to OD₆₀₀ = 1) were spotted on plates and grown for 2.5 days at 30°C. **(D)** Expression levels of Wss1 variants used in **(C)**. Extracts of exponentially grown cells prepared using the TCA method were analyzed by immuno-blotting using HA-specific antibodies. Dpm1 levels serve as loading control. **(E)** Five-fold serial dilutions of cells grown over night (adjusted to OD₆₀₀ = 1) were spotted on YEP plates either containing 1% DMSO or 1% DMSO and 30 μ M CPT. Plates were incubated at 30°C for 2.5 days.

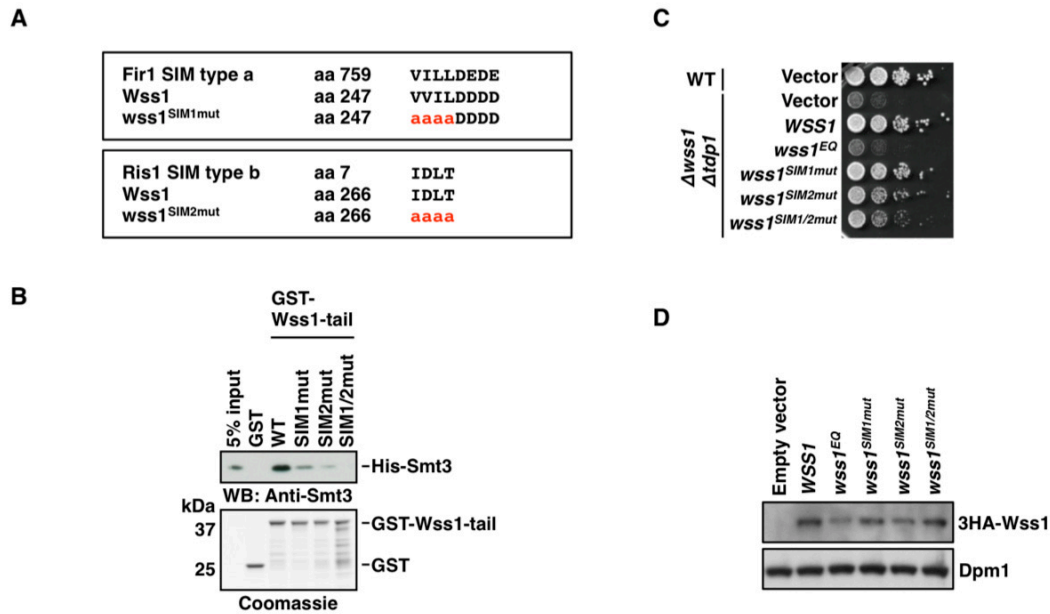


Figure 9. Wss1 binding to SUMO supports its function. (A) Wss1 contains two SIMs (one type a and one type b SIM). Sequences of SIMs within Wss1 are presented together with sequences of canonical SIMs. Amino acid replacements in Wss1 variants are highlighted in red. **(B)** Interactions of GST-tagged Wss1 fragments with His-tagged Smt3 were tested by GST pull-down assays. GST or GST-tagged Wss1 fragments were coupled to GSH-Sepharose and incubated together with recombinant His-tagged Smt3. Samples were incubated for 1 hr at 4°C prior to several wash steps and analysis by SDS-PAGE followed by either Coomassie-blue staining or immuno-blotting using Smt3-specific antibodies. **(C)** Complementation of $\Delta wss1 \Delta tdp1$ cells with 3HA-tagged Wss1 variants with altered SIMs. Five fold serial dilutions of cells were spotted on plates and grown for 2.5 days at 30°C. **(D)** Expression levels of Wss1 variants used in **(C)**. Extracts of exponentially grown cell prepared using the TCA method were analyzed by immuno-blotting using HA-specific antibodies. Dpm1 levels serve as loading control.

segregase Cdc48 were identified (Figure 8A), one of which, a so called VCP-interacting motif (VIM) has also been predicted by a bioinformatic approach (Stapf et al., 2011). The other motif represents a SHP-box, which is found for example in the canonical Cdc48 binding protein Shp1 (Stolz et al., 2011). Wss1 variants with internal deletions of these motifs were found to be deficient in Cdc48 binding and are non-functional (PhD thesis M. Schwarz). As deletions carry the risk of resulting in general structural alterations, point mutants in these motifs were constructed to confirm a joint function of Wss1 and Cdc48 (Figure 8A). Changes in only one of the Cdc48-binding motifs do not affect the binding of Wss1-fragments to Cdc48, as judged by GST pull-down assays. Wss1-fragments with amino acid replacements in both Cdc48 interaction motifs ($wss1^{\text{SHP/VIMmut}}$) however exhibit strongly reduced binding to Cdc48 (Figure 8B). Consistent with previous results this variant fails to complement the slow growth of $\Delta wss1 \Delta tdp1$ cells (Figure 8C-D), indicating that Cdc48 binding is indeed essential for Wss1's function *in vivo*. Notably, already alterations in the SHP-box

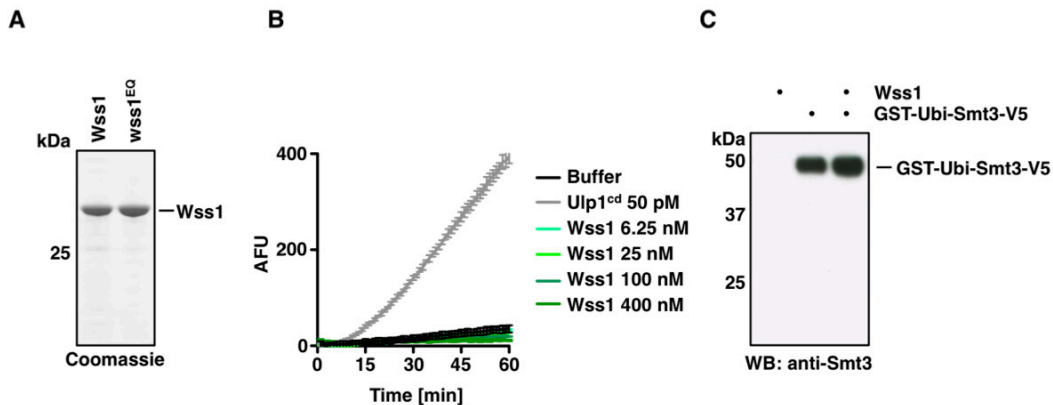


Figure 10. Wss1 is not a SUMO-dependent isopeptidase. (A) SDS-PAGE of purified recombinant Wss1 (wildtype and wss1-EQ) expressed in *E. coli* cells. (B) Wss1 was tested for SUMO isopeptidase activity using the commercial Smt3-CHOP assay. The Smt3-CHOP assay measures the cleavage of Smt3 linearly fused to a reporter enzyme, which is inactive as a fusion. Cleavage by an isopeptidase renders the reporter active, thus resulting in the production of a fluorescent substrate. The produced fluorescence correlates directly with the cleavage of the Smt3-reporter fusion and therefore with SUMO-isopeptidase activity. The assay was performed using several concentrations of Wss1 (6.25 - 400 nM). The catalytic domain of the canonical yeast SUMO isopeptidase Ulp1 (Ulp^{cd} - 50 pM) served as a positive control. (C) A GST-Ubi-Smt3-V5 fusion is not cleaved by Wss1. GST-Ubi-Smt3-V5 was incubated alone or together with Wss1 for 2 hrs at 30°C prior to SDS-PAGE and analysis by immuno-blotting using Smt3-specific antibodies.

(*wss1*^{SHPmut}) lead to a partial defect in complementation whereas *in vitro* binding seems unaffected, indicating that the two Cdc48 interaction motifs are at least *in vivo* not fully redundant. The requirement for functional Cdc48 interaction motifs in Wss1 implicates that also Cdc48 function itself should become important in the absence of Tdp1. Indeed, cells with compromised Cdc48 function (*cdc48-6*) become significantly more CPT sensitive, if lacking Tdp1 in addition. In contrast, deletion of *WSS1* in *cdc48-6* cells has no effect (Figure 8E). We conclude that Wss1 and Cdc48 are jointly required to counteract Top1ccs in a pathway parallel to Tdp1.

3.2.2 Wss1 function is linked to the SUMO system

In addition to Cdc48 interaction, the C-terminal tail of Wss1 harbors two canonical SIMs (SUMO-interaction motifs) required for binding the ubiquitin-like protein SUMO (Mullen et al., 2010). Thus, we tested if SUMO (Smt3 in yeast) binding is essential for Wss1's function. To this end, we constructed Wss1 variants in which crucial SIM residues were replaced by alanine (Figure 9A). Changing either SIM in Wss1 reduces SUMO binding by Wss1, as judged by GST-pulldown assays, but variants with changes in both SIMs (*wss1*^{SIM1/2mut}) are completely defective in SUMO binding (Figure 9B). However, *in vivo* they were at least partially able to complement the loss of Wss1 (Figure 9C-D). Given the fact that Wss1 was described as an unusual

SUMO-dependent isopeptidase (Mullen et al., 2010), this was an unexpected result, as one would assume that such an activity would be entirely dependent on SUMO recognition. Isopeptidases are enzymes able to cleave isopeptide bonds. For example, de-ubiquitylation and de-sumoylation reactions are catalyzed by isopeptidases, which cleave the isopeptide bond between the terminal diglycine of ubiquitin-like proteins and the substrate's acceptor lysine. As it was unclear how the proposed SUMO-dependent isopeptidase activity was related to our findings, we initially attempted to reproduce the reported findings. We assessed SUMO-dependent isopeptidase activity of recombinantly expressed Wss1 with the commercial Smt3-CHOP assay system (Figure 10A). In this assay, SUMO isopeptidase activity is measured by the cleavage of a linear Smt3-reporter fusion (the reporter enzyme is inactive as a fusion). Cleavage of the fusion protein allows the production of a fluorescent substrate, which is detected in real-time with a multiplate fluorescence reader. Surprisingly, we were not able to detect any SUMO isopeptidase activity in our Wss1 preparations (Figure 10B). Additionally, we tested cleavage of a GST-Ubi-Smt3-V5 fusion, exactly as reported (Mullen et al., 2010). Again, we did not observe any cleavage by Wss1 (Figure 10C). It should be noted that the biochemical experiments presented in Mullen et al. raised several questions, given that (1) the observed activity remained active in the presence of EDTA, (2) a variant with alterations in three active site residues retained partial activity and (3) that activity was inhibited by ubiquitin-aldehyde, a classical inhibitor of thiol-based ubiquitin-isopeptidases. Generally, all these biochemical observations are consistent with the possibility that the observed activity arose from a contamination in the Wss1 preparation, as noted previously (Su and Hochstrasser, 2010). Together with the findings that our Wss1 preparations were active in the experiments discussed later, were inhibited by EDTA and a variant with replacements of active site residues (wss1^{EQ}) showed no activity, we conclude that Wss1 is most likely not a SUMO-dependent isopeptidase.

3.3 Wss1 is a DNA-dependent protease

The finding that Wss1 is not an isopeptidase raised the exciting hypothesis that Wss1 might in fact act directly and proteolytically on Top1ccs, thereby diminishing their toxicity. Indeed, Wss1 is able to cleave epitope-tagged Top1, which was immuno-purified from yeast cells (PhD thesis M. Schwarz and Figure 11A upper panel). However, cleavage does not take place when EDTA is included in the reaction or when the catalytic inactive variant $wss1^{EQ}$ is used. Furthermore, not only Top1 is cleaved in this reaction, but also Wss1 itself (Figure 11A, lower panel). This was very surprising to us, given the fact that Wss1 incubated alone (without Top1 immuno-precipitate) does not undergo self-cleavage (Figure 11B, left lanes), implicating that some factor within the Top1 immuno-precipitate induces Wss1 self-cleavage.

To gain more insights into the function of Wss1 we decided to further characterize the requirements for self-cleavage. Surprisingly, we found that already the addition of a whole cell extract to Wss1 is enough to trigger self-cleavage (Figure

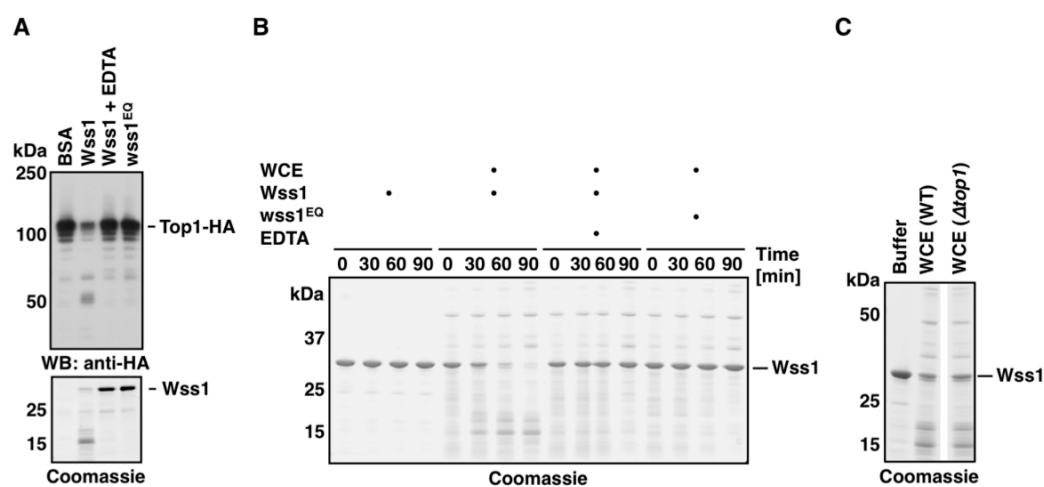


Figure 11. Wss1 cleaves Top1 and itself. (A) HA-tagged Top1 was purified from yeast cells by immuno-precipitation using HA-specific antibodies. Immuno-precipitated Top1 was then incubated with either BSA, Wss1, Wss1 and EDTA (10 mM) or $wss1^{EQ}$ for 2 hrs at 30°C. Reactions were stopped by addition of Laemmli buffer and analyzed by SDS-PAGE either followed by immunoblotting using HA-specific antibodies (upper panel) or Coomassie staining (lower panel). **(B)** Wss1 (in the absence or presence of EDTA (10 mM)) or its catalytic inactive variant were either incubated alone (only for Wss1 without EDTA) or in the presence of whole cell extract for the indicated time at 30°C. Reactions were stopped by the addition of Laemmli buffer and cleavage was analyzed by SDS-PAGE followed by Coomassie staining. Whole cell extract was prepared from exponentially growing WT cells using a bead beater. **(C)** Wss1 was incubated alone or together with cell extract prepared from either WT or $\Delta top1$ cells for 45 min at 30°C. Reactions were stopped by the addition of Laemmli buffer and analyzed by SDS-PAGE followed by Coomassie staining. Samples were run on the same gel; irrelevant lanes were removed as indicated by white spacer.

11B). Importantly, the observed cleavage is dependent on Wss1's catalytic activity as, it is inhibited by EDTA and not seen with the catalytic inactive variant wss1^{EQ}. Top1 itself could be excluded as the factor responsible for cleavage induction, as extracts from cells lacking Top1 ($\Delta top1$) induce cleavage to the same extent as

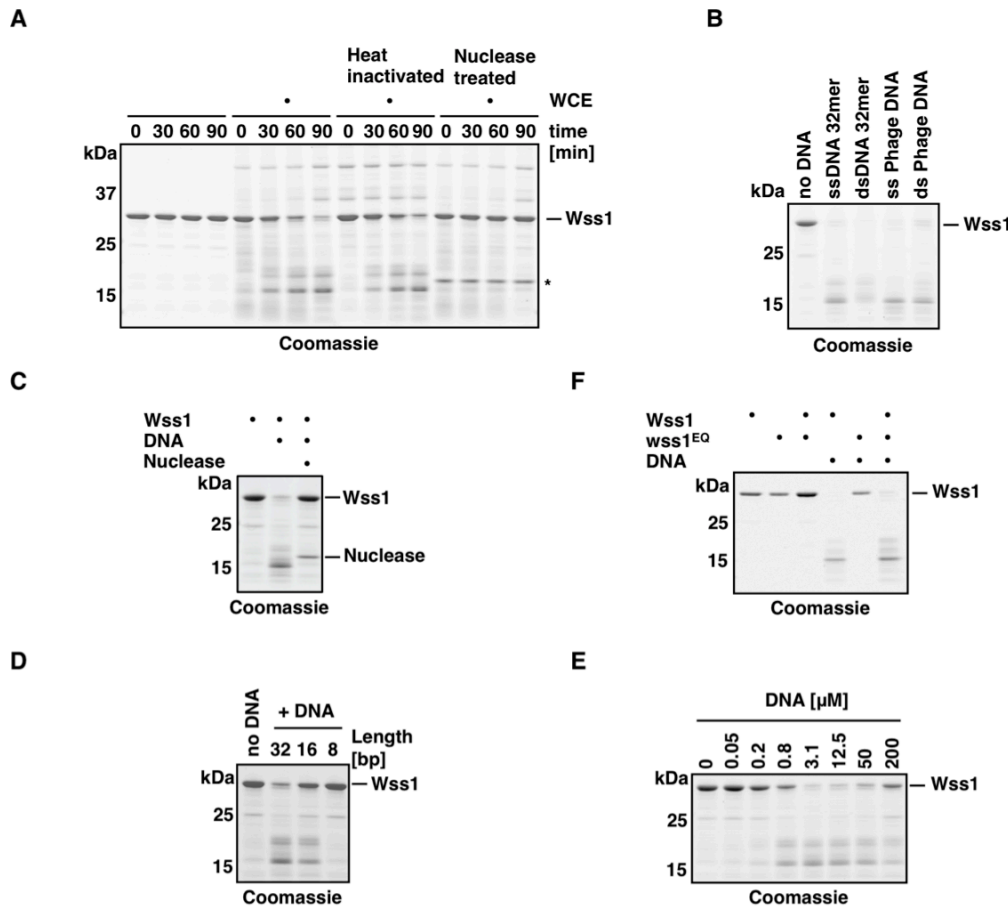


Figure 12. Wss1 is a DNA-dependent protease. (A) WCE heat inactivated at 80°C for 20 min induces Wss1 self-cleavage. In contrast, WCE subjected to nuclease digestion completely fails to induce self-cleavage (asterisks denotes the nuclease). Wss1 was either incubated alone or with the respective WCE (untreated, heat-inactivated or nuclease treated). Reactions were stopped by addition of Laemmli buffer at the indicated time points and analyzed by SDS-PAGE and Coomassie-blue staining. (B) Various types of DNA induce Wss1 self-cleavage. Wss1 (200 ng/ μ l) was incubated alone or together with different types of DNA (32 bp oligonucleotides or phage Φ X174 DNA, both single- (50 ng/ μ l) and double-stranded (100 ng/ μ l)). Reactions were carried out at 30°C for 2 hrs prior to SDS-PAGE and Coomassie-blue staining. (C) DNA polymers are required for induction of self-cleavage. Wss1 was either incubated alone, with DNA (Φ X174 virion) or with DNA predigested with nuclease for 2 hrs at 30°C. Cleavage reactions were analyzed by SDS-PAGE followed by Coomassie-blue staining. (D) A minimal DNA length is required to induce Wss1 self-cleavage. Wss1 (50 ng/ μ l) was incubated together with DNA oligonucleotides (20 μ M) of different lengths for 1 hr at 30°C, prior to analysis by SDS-PAGE and Coomassie-blue staining. (E) Equimolar concentrations of DNA are most efficient in inducing Wss1 self-cleavage. Wss1 (6.6 μ M) was incubated with different amounts of DNA (32 bp single stranded oligonucleotide) for 1 hr at 30°C. (F) Wss1 self-cleavage occurs *in trans*. Wss1 and its inactive variant wss1^{EQ} (50 ng/ μ l) were either incubated alone or together with and without DNA (Φ X174 virion, 100 ng/ μ l). Reactions carried out at 30°C for 2 hrs and analyzed by SDS-PAGE and Coomassie-blue staining.

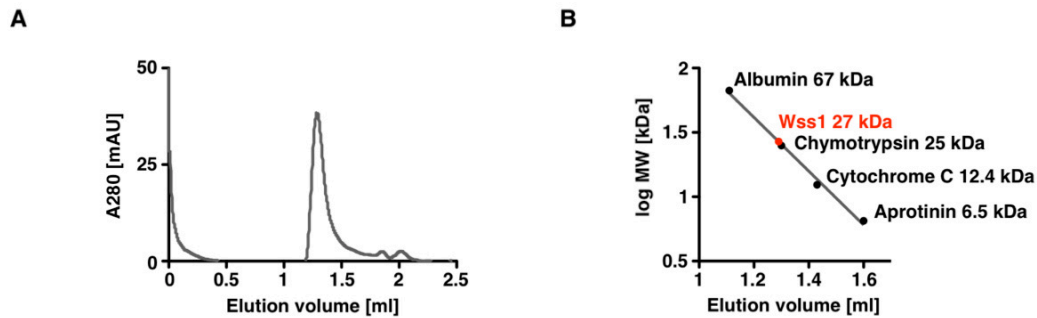


Figure 13. Wss1 is a monomeric protein. (A) Size exclusion chromatography was carried out on Superdex75 column employing the same buffer conditions used in cleavage experiments. (B) Elution volumes of proteins used to calibrate the sizing column. The molecular weight calculated for the elution volume of Wss1 in 27 kDa, closely matching the predicted molecular weight of 30.6 kDa.

extracts from WT cells (Figure 11C). Intriguingly, even cell extracts heat-inactivated for 20 min at 80°C (thereby inactivating all protein components) potently induce self-cleavage. By contrast, digestion of the cell extract with micrococcal nuclease abolishes cleavage induction entirely (Figure 12A). As Wss1 presumably acts on Top1 trapped on DNA we speculated that DNA might be the crucial component responsible for induction of Wss1 self-cleavage. Indeed, addition of various types of DNA is sufficient to induce self-cleavage of Wss1 (Figure 12B). Notably, intact DNA polymers are required to induce self-cleavage, as DNA predigested with nuclease fails to induce cleavage (Figure 12C). More precisely, a certain DNA length is needed for cleavage induction, as 8 bp oligonucleotides fail to induce cleavage, whereas 16 and 32 bp oligonucleotides potently do (Figure 12D). Furthermore, equimolar amounts of DNA are most efficient in inducing self-cleavage, whereas very high concentrations are inhibitory (Figure 12E). In addition, self-cleavage occurs *in trans*, which we deduce from the fact, that the catalytic inactive variant $wss1^{EQ}$ is cleaved when WT enzyme is present in the reaction. Notably, self-cleavage is entirely dependent on the presence of DNA (Figure 12E).

Taken together, we conclude that DNA induces self-cleavage by acting as a scaffold bringing to Wss1 molecules in close proximity, thereby enabling cleavage *in trans*. This model explains why a certain DNA length is required (long enough to harbor two Wss1 molecules) and why high DNA concentrations are inhibitory (as all Wss1 molecules will be titrated away from each other). An alternative model, in which the proteolytic activity of a constitutive Wss1 dimer is activated by DNA, can be excluded, as Wss1 behaves as a monomer under conditions in which the cleavage assays are performed (Figure 13A-B).

3.4 Wss1 targets DNA-bound proteins

3.4.1 Wss1 is a DNA-binding protein

The idea that DNA induces Wss1 self-cleavage by acting as a scaffold implicates that Wss1 is a DNA-binding protein. However, no DNA-binding domain has been described or predicted for Wss1 so far. Thus, we directly tested DNA-binding by using GST-tagged fragments of Wss1's C-terminal tail (Figure 14A) in an

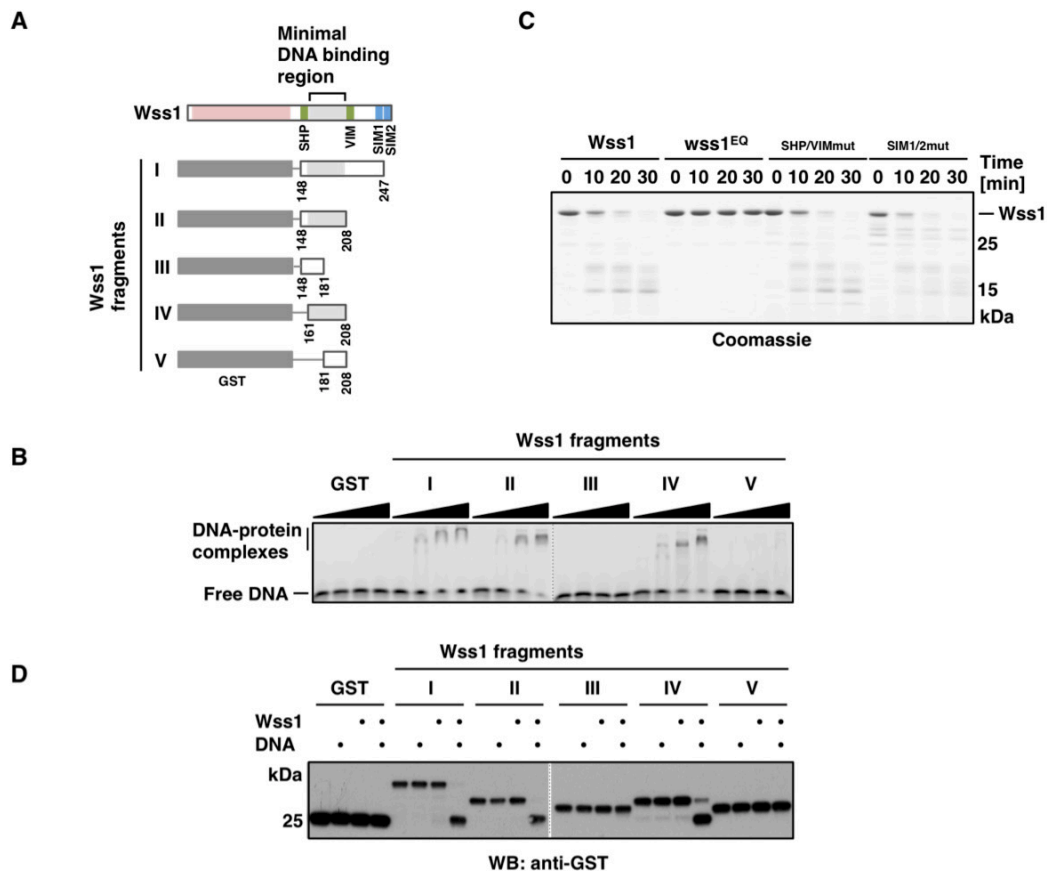


Figure 14. Wss1 contains a DNA-binding domain. (A) Schematic depiction of Wss1 and GST-tagged Wss1 fragments used for mapping of Wss1's DNA binding domain (light gray indicates the region minimally required for DNA-binding) (B) Wss1 bears a DNA-binding domain. Different concentrations of GST-tagged fragments of Wss1's C-terminal tail (0.16, 0.8, 4 and 10 μ M) were incubated together with Alexa488-labeled double stranded DNA oligonucleotides (0.1 μ M) for 20 min at room temperature prior to separation on 6 % DNA retardation gels. Mobility shifts were visualized using a fluorescence scanner. Samples were run in parallel on two separate gels, as indicated with the dotted line. (C) Wss1 variants deficient in Cdc48 or SUMO binding are not affected in their DNA-dependent proteolytic activity. Wss1 and the respective variants were incubated together with DNA (Φ X174 virion) at 30°C. The reactions were stopped at the indicated time points by addition of Laemmli buffer. Cleavage was analyzed by SDS-PAGE followed by Coomassie-blue staining. (D) Wss1 cleaves DNA-bound GST-tagged Wss1-fragments. Wss1-fragments were incubated either alone or with full-length Wss1 in the absence or presence of DNA (Φ X174 virion) for 2 hrs at 30°C. Reactions were stopped by the addition of Laemmli buffer and analyzed by immuno-blotting using GST-specific antibodies.

electrophoretic mobility shift assay (EMSA). DNA-binding, as inferred from the ability to retard a fluorescently labeled double-stranded oligonucleotide during electrophoresis, was readily detectable in Wss1's tail. The DNA-binding domain of Wss1 could be mapped to a region ranging from amino acid 161 to 208 located directly between the Cdc48 interaction motifs (Figure 14B). To exclude that the aforementioned alterations in the Cdc48 interaction motifs also affected DNA binding, we tested the DNA-dependent proteolytic activity of Wss1 variants with amino acid replacements in either both Cdc48 interaction motifs or both SIMs. However, neither of these variants display altered induction of DNA-dependent self-cleavage, indicating that alterations in the Cdc48 interaction motifs or SIMs do not affect DNA-binding or catalytic activity (Figure 14C).

As Wss1 is able to cleave another Wss1 molecule in the presence of DNA, we next asked if this is also the case for Wss1-fragments. Therefore, we incubated the Wss1 fragments used for DNA-binding analysis together with full length Wss1 in the absence or presence of DNA. Astonishingly, only those Wss1 fragments able to bind DNA were cleaved by full length Wss1. Importantly, cleavage was strictly dependent on the presence of DNA (Figure 14D). This further indicates that DNA enables cleavage by Wss1 by acting as a scaffold bringing the enzyme and its substrate (in this case the Wss1-fragments) together. The fact that fragments without DNA-binding properties are not cleaved is actually expected from the scaffolding model, as they will not co-localize together with Wss1 on DNA.

3.4.2 Wss1 cleaves DNA-binding proteins

Wss1's ability to cleave specifically DNA-bound fragments lead to the hypothesis that other DNA-bound proteins might be substrates as well. As Wss1 presumably acts on Top1 covalently trapped on DNA, we asked whether cleavage of Top1 by Wss1 also occurs in a DNA-dependent manner.

Indeed, we observed cleavage of recombinant Top1 (commercially available human Top1 purified from insect cells was used; functionally equivalent to yeast Top1 (Bjornsti et al., 1989)) when incubated together with catalytically active Wss1 (Figure 15A). Importantly, this is strictly dependent on the presence of DNA, as no cleavage fragments is observed when DNA is omitted from the reaction. To gain more insights into the specificity of Wss1, we repeated this assay by replacing Top1 with other proteins. Initially we focused on other DNA-binding proteins. Surprisingly, all DNA-binding proteins tested, such as histone H1 or Hmg1, are cleaved by Wss1 in a strictly DNA-dependent manner (Figure 15B-C). This in stark contrast to proteins

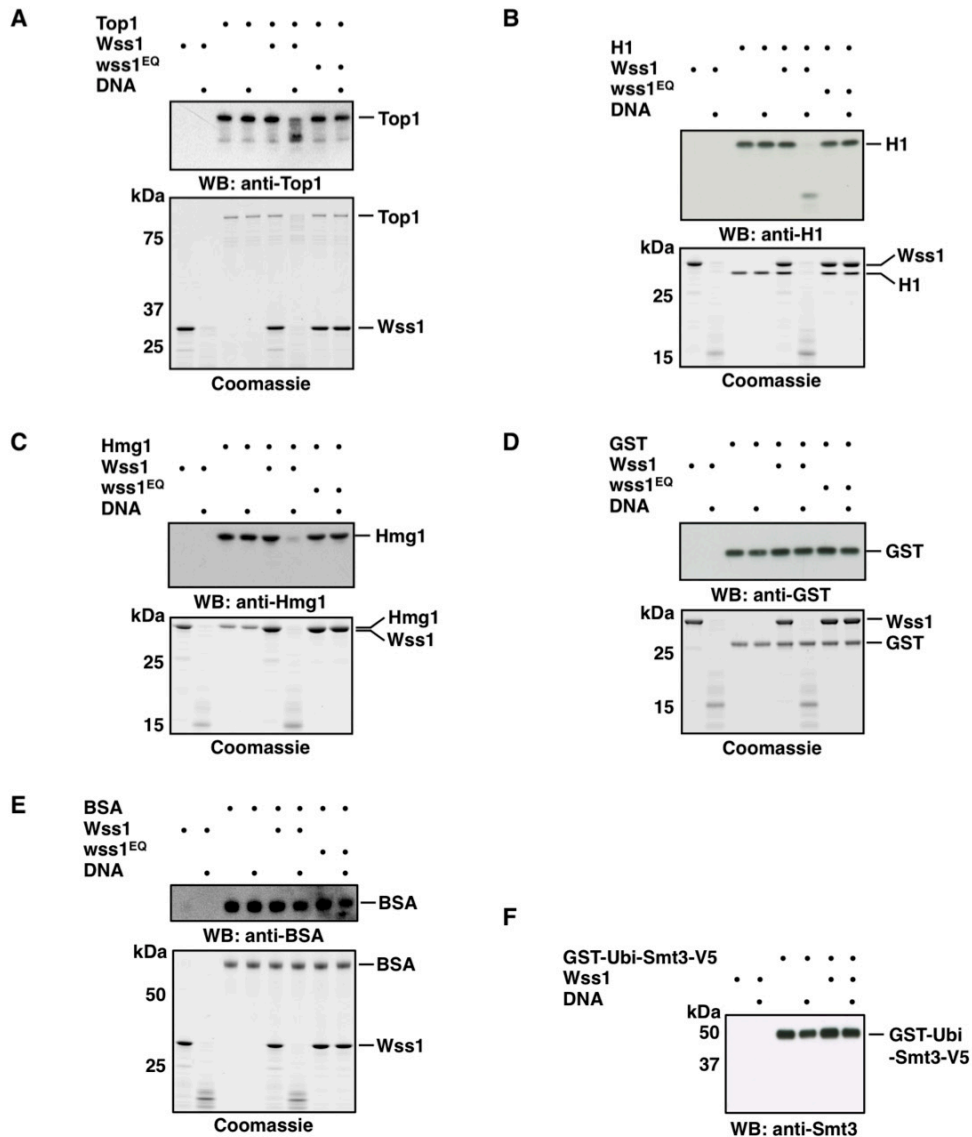


Figure 15 Wss1 targets specifically DNA-bound proteins. Topoisomerase 1 (A), histone H1 (B), Hmg1 (C), GST (D), BSA (E) or a GST-Ubi-Smt3-V5 fusion (F) were incubated either alone or together with Wss1 or its inactive variant wss1^{EQ} (F) only with Wss1) either in the presence or absence of DNA (Φ X174 virion). Reactions were carried out at 30°C for 2 hrs and were stopped by the addition of Laemmli buffer. Proteolytic cleavage was analyzed by SDS-PAGE followed by Coomassie-blue staining (not in (F)) as well as by immuno-blotting using substrate-specific antibodies.

without DNA-binding capabilities (BSA, GST or the aforementioned GST-Ubi-Smt3-V5 fusion), which are not cleaved by Wss1, even when DNA is present in the reaction (Figure 15D-F).

Taken together, these data suggest that Wss1 is able to cleave any protein (irrespective of identity and amino acid sequence) with DNA-binding properties in the presence of DNA. This is probably because in the presence DNA both substrate and Wss1 might bind the same DNA molecule, thereby bringing them in close proximity

and thus enabling proteolysis. The *in vitro* promiscuity of Wss1, however, remained puzzling and indicated that Wss1 might target also *in vivo* a broader set of substrates than initially anticipated.

3.5 Wss1 is involved in cellular resistance towards formaldehyde

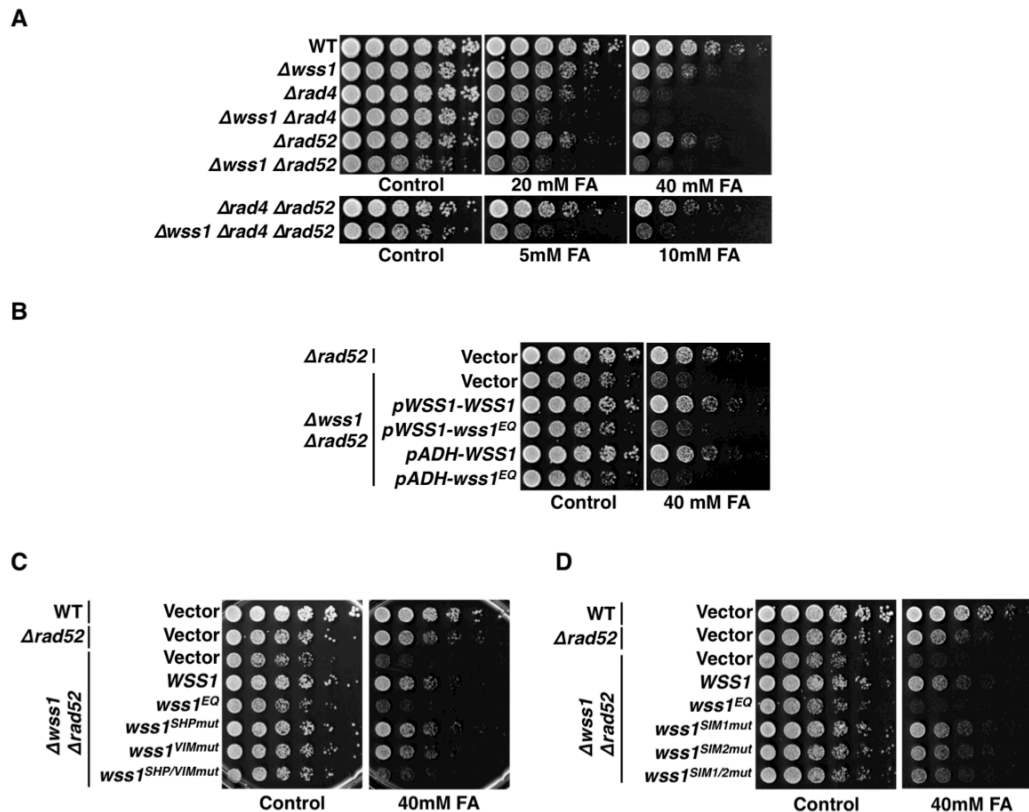
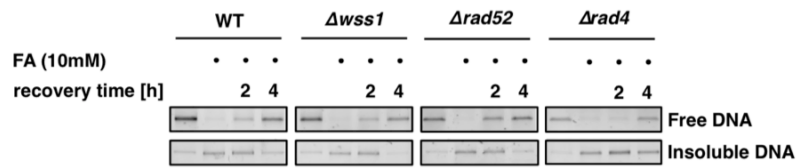


Figure 16. Wss1 is needed for FA resistance. (A) Wss1 is needed for cellular resistance towards FA and operates independent of NER or HR. WT strain or strains lacking Wss1, Rad4, Rad52 or combinations were washed once in PBS and incubated in PBS containing the respective FA concentration for 15 min under constant shaking. Following two wash steps cells were then spotted in five-fold serial dilutions on YPD plates and incubated at 30°C for 2.5 days. (B) Wss1's proteolytic activity is required for FA-resistance. Cells lacking Rad52 and Wss1 were complemented with plasmids coding for HA-tagged Wss1 or *wss1*^{EQ} either under control of the endogenous promoter or the *ADH* promoter (causing heavy over-expression). FA treatments and spottings were performed as in (A). (C-D) Cdc48 binding is essential and SUMO binding is supportive for Wss1's function in FA resistance. Cells lacking Rad52 and Wss1 were complemented with plasmids coding for the indicated HA-tagged Wss1 variants. FA treatments and spottings were performed as in (A).

DPCs are not only caused by the malfunctioning actions of topoisomerases and relatives, they are also induced by nonenzymatic reactions. Agents causing DPCs nonenzymatically are amongst others IR, UV-light and reactive aldehydes (see Introduction) (Barker et al., 2005). Among reactive aldehydes, formaldehyde (FA) is of explicit interest given the fact that it is produced endogenously directly within chromatin during every histone de-methylation event (Kooistra and Helin, 2012).

A



B

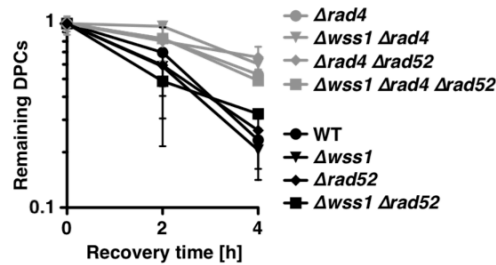


Figure 17. Bulk repair of FA-induced DPCs is cleared by NER. (A) Direct measurements of FA-induced DPC repair. Yeast cells (untreated or treated with 10 mM FA (with or without recovery time in FA free media)) were lysed by zymolase treatment and addition of SDS. Proteins were precipitated from the lysate by addition of KCl. Free DNA (meaning not crosslinked to protein) remained in the supernatant. The protein precipitate was washed several times prior to removal of proteins by proteinase K digestion and quantification of the insoluble DNA (DNA crosslinked to protein). **(B)** Quantification of DPC-repair assays as shown in **(A)**. The ratio between insoluble DNA and total DNA (soluble + insoluble) served as a measure of DPCs. Values of each experiment were normalized to the 0 hr time point. DPC levels are depicted on a \log_{10} scale as mean values \pm SD of 2 - 4 independent experiments. DPC levels of yeast cells lacking NER ($\Delta rad4$) are presented in light gray whereas NER proficient cells in black.

Therefore, we decided to use FA-induced DPCs as a model to study a potential involvement of Wss1 with respect to the repair of nonenzymatic DPCs. To this end, we challenged WT strains and strains lacking Wss1 ($\Delta wss1$) with a short (15 min) FA pulse to induce DPCs. After removing FA by two wash steps, cells were spotted on plates and incubated for 2.5 days at 30°C. Cells lacking Wss1 indeed displayed significant sensitivity towards FA (Figure 16A). So far only the canonical DNA repair pathways homologous recombination (HR) and nucleotide excision repair (NER) had been implicated in the response to FA-induced DPCs in yeast (de Graaf et al., 2009). To test if Wss1's function is integrated into one of these pathways we performed epistasis analysis with deletions in NER ($\Delta rad4$) or HR ($\Delta rad52$). If Wss1 would be part of either pathway, a deletion of WSS1 is expected to not further increase the sensitivity of cells lacking that specific pathway. However, the additional deletion of WSS1 in cells lacking NER, HR or both, increased in all cases FA sensitivity markedly (Figure 16A), indicating that Wss1 constitutes a third and novel mechanism required for resistance towards FA-induced DPCs. The requirements for Wss1 in FA-resistance seem analogous to the ones needed for its function in Top1cc repair. The catalytic inactive variant $wss1^{EQ}$ does not complement the strong FA sensitivity of

Δrad52 Δrad4 cells, even when heavily overexpressed (Figure 16B). Cdc48 interaction also appears to be essential, as a Wss1 variant with both Cdc48-interaction motifs altered (*wss1^{SHP/VIMmut}*) fails to rescue the knockout phenotype entirely (Figure 16C). In contrast, SUMO binding seems to be only partially required for function, as similarly observed for Top1cc repair, as variants with both SIMs mutated (*wss1^{SIM1/2mut}*) still complement the knockout to a certain degree (Figure 16C-D). To further understand Wss1's contribution to FA resistance, we next performed assays monitoring directly the repair of FA-induced DPCs, which quantify the amount of DNA co-precipitating with protein under denaturing conditions. The assay was adapted from previously published methods, however, with some modifications (de Graaf et al., 2009). In brief (see Materials and Methods for details), cells from exponentially growing cultures were washed once in PBS, followed by a FA exposure (10 mM in PBS, 15 min) to induce DPCs. Cells were subsequently washed twice in PBS to remove excess FA and resuspended in fresh warm media. Cells were either harvested immediately or incubated at 30°C to allow for repair of DPCs (2 or 4 hrs). At the respective timepoints, cells were harvested, washed and subjected to zymolase treatment (which degrades the cell wall), followed by cell lysis with SDS (also denaturing all protein components and thus removing all non covalent attached proteins from DNA). Next, proteins were precipitated from the lysate by

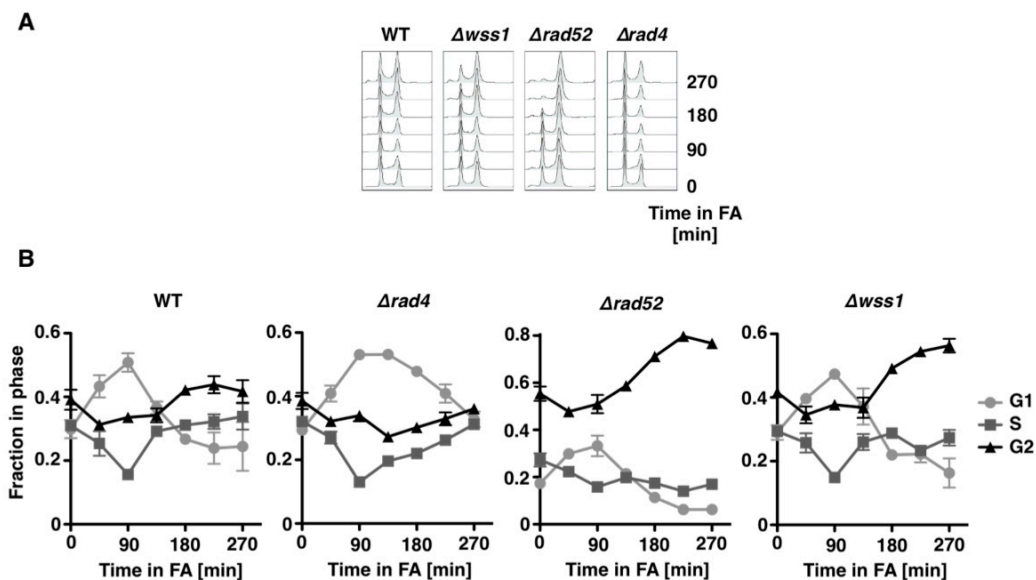


Figure 18. Cells lacking Wss1 or HR arrest specifically with a G2-like DNA content upon FA exposure. (A) FA was added to exponentially growing cells to a final concentration of 0.75 mM. Samples were harvested every 45 min and cell cycle profiles analyzed by SYTOX green staining and flow cytometry. (B) Quantification of cell cycle phase distribution over time after FA addition of two independent experiments \pm SD (one replicate is shown in (A)).

addition of KCl. This was followed by centrifugation in order to pellet all protein, whereas DNA was expected to remain in the supernatant (the supernatant was saved to quantify the amount of soluble DNA). Next, the protein pellet was dissolved and re-precipitated several times, to ensure that all free DNA was removed from the precipitate. Finally, proteins were removed by proteinase K. The amount of insoluble DNA (co-precipitated in the protein pellet) and soluble DNA was now quantified by agarose gel electrophoresis. The ratio between insoluble DNA versus total DNA (insoluble and soluble) served as a measure for the amounts of DPCs. In this assay, WT cells repair 80 - 90% of FA-induced DPCs over the course of 4 hrs. Surprisingly, cells lacking Wss1, HR ($\Delta rad52$) or both repair DPCs with the same kinetics as WT cells do (Figure 17A-B). The only strains displaying a delay in the removal of DPCs are cells lacking NER ($\Delta rad4$).

This finding was unexpected as especially $\Delta wss1 \Delta rad52$ cells are extremely sensitive towards FA, notably even more than $\Delta rad4$ cells (Figure 16A). As a consequence, it seems that the FA sensitivity observed in cells lacking Wss1 or HR does not arise from a defect in bulk repair of DPCs. We reasoned that Wss1 or HR might target a special class of DPCs - highly toxic, however, small in numbers - thereby invisible in our assays. HR is known to be crucial for repair/tolerance of DNA damage during S-phase and our data indicated that Wss1 is required for suppressing Top1cc-dependent cell cycle defects. Thus, we speculated that this toxic class of DPCs might in fact consist of DPCs causing problems in S-phase (possibly through replication fork stalling). To test this hypothesis we analyzed the effects on the cell cycle status upon FA exposure in WT cells and cells lacking Wss1, HR or NER (Figure 18A). The quantification of cell cycle phase distributions over time (Figure 18B) revealed a specific pattern in WT cells, which is characterized by an initial drop in S-phase cells accompanied by a reciprocal increase in G1 cells, followed by a reversion to the levels seen in unchallenged cells (Figure 18B, left panel). Cells lacking NER ($\Delta rad4$) display a similar response (decrease in S-phase, increase in G1-phase cells), however with a strong delay. By contrast, cells lacking HR ($\Delta rad52$) or Wss1 display an initial response identical to that seen in WT cells (consistent with the observation, that bulk DPC repair is functional), which is, however, followed by a specific accumulation of cells with a G2-like DNA content (Figure 18B, right panels). This indicates that cells lacking HR or Wss1 indeed suffer from cell cycle defects upon FA exposure despite being competent in repairing the bulk of DPCs. We assume that the observed cell cycle arrest is likely responsible for the strong

sensitivity seen in these strains. Taken together, we conclude that the bulk of DPCs are repaired by NER, whereas HR and Wss1 constitute equally important mechanism required to prevent specific cell cycle defects linked to DPCs, which remained unrepaired until S-phase.

3.6 Wss1-dependent DPC-processing directs repair pathway choice

Cells lacking both Wss1 and HR ($\Delta wss1 \Delta rad52$) are significantly more FA sensitive than the respective single mutants (Figure 16A), indicating that HR and Wss1 are parallel mechanisms needed for cellular FA resistance. As a matter of fact, $\Delta wss1$ cells had previously been found in a screen to exhibit increased levels of GFP-Rad52 foci, a marker for sites of active recombination (Alvaro et al., 2007). To directly test if recombination is more active in cells lacking Wss1 we performed interchromosomal recombination assays. This assay measures the frequency of recombination events in diploid cells carrying two non-functional *HIS1* alleles (*his1-1* and *his1-7*, each allele bearing a different inactivating mutation) located on two different chromosomes (Pfander et al., 2005). These cells are unable to grow on media lacking histidine (SC-HIS), unless a recombination event occurred between the two non-functional alleles resulting in a functional *HIS1* gene. To quantify these events, fluctuation analysis was performed in order to measure recombination rates, i.e. the likelihood of a recombination event per cell division. (Lea and Coulson, 1949; Luria and Delbrück, 1943). To this end, liquid cultures were inoculated with a small number of cells, which were then grown for three days. During the incubation time recombination events can occur resulting in cells auxotrophic for histidine. The frequency of histidine auxotrophic mutants per total viable cell number was determined in 8 - 10 parallel cultures by plating fractions of the culture on plates lacking histidine as well as on non-selective plates. Recombination rates were then calculated from mutant frequencies by a maximum-likelihood approach using the FALCOR web-tool (Hall et al., 2009). Cells lacking Wss1 show indeed increased recombination levels (Figure 19A), further indicating a parallel and partial redundant role of Wss1 and recombination. To test if the observed increase in recombination rates is linked to DPC repair we also assayed recombination rates with cells being cultured in the presence of FA.

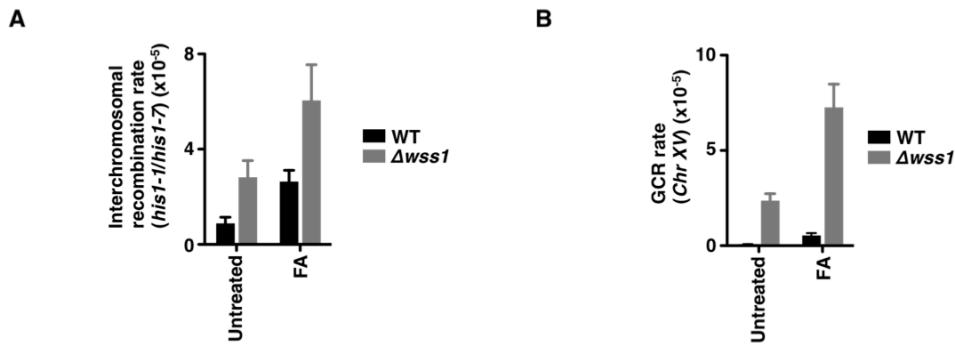


Figure 19. Cells lacking Wss1 display increased recombination levels and suffer from genomic instability. (A) Interchromosomal recombination rates are higher in cells lacking Wss1 and are even further increased upon FA exposure. Recombination rates between the two non-functional hetero-alleles *his1-1* and *his1-7* were determined in diploid cells using fluctuation analysis. Fluctuation tests were performed using at least 8 parallel cultures per strain and condition grown for 3 d at 30°C. FA-induced recombination levels were measured by addition of 1 mM FA to the growth media. Recombination rates are represented as mean values of three independent experiments. Error bars indicate standard deviations. **(B)** Wss1 suppresses genomic instability especially in cells challenged by FA. GCR rates were determined by fluctuation test using at least 8 parallel cultures. FA-induced GCR events were measured by addition of 1 mM FA to the growth media. The presented GCR rates are mean values of 2 - 4 independent experiments. Error bars indicate standard deviations.

Again, the increase in recombination upon FA exposure was clearly more pronounced in cells lacking Wss1 (Figure 19A). Recombination is a powerful DNA repair mechanism bearing, however, the risk of genomic rearrangements and other alterations (Mieczkowski et al., 2006). In fact, *WSS1* had already been identified in a screen as a suppressor of gross chromosomal rearrangements (GCRs) (Kanellis et al., 2007). In this study, GCRs were measured as the frequency by which the terminal part of the left arm of chromosome XV was lost. Two counter-selectable markers (*URA3* and *CAN1*) were introduced into the sub-telomeric region of Chr XV. Cells bearing both markers are sensitive to 5-Fluoroorotic acid (5'FOA) and canavanine. This allows the identification of cells, which have lost this arm of Chr XV, as these cells will be resistant to both, 5'FOA and canavanine. The frequency of GCR events can again be scored by fluctuation analysis in an approach similar to the one described for recombination events. We reconstructed this GCR assay system in our yeast background (the construction and GCR experiments were performed in collaboration with N. Blömeke and were already partially described in the bachelor thesis of N. Blömeke) and could indeed confirm the function of *WSS1* as a GCR suppressor (Figure 19B and bachelor thesis N.Blömeke). Notably, GCR rates in cells lacking Wss1 were even more induced if the cells were cultivated in the presence of FA (Figure 19B), further confirming that cells deficient for Wss1 rely on recombinational repair to handle DPCs resulting in genomic rearrangements and

instability. Moreover, this finding provides additional support for a model in which Wss1 targets specifically DPCs causing replication problems in S-phase, as GCR events are thought to be primarily caused by permanent replication fork stalling (Lambert et al., 2005).

In general, DNA lesions inhibiting replisome progression are not only handled by HR, but also by postreplicative repair mechanisms (PRR). Upon replication fork stalling, mono- or poly-ubiquitylation of PCNA triggers PRR (Hoege et al., 2002). Mono-ubiquitylation of PCNA recruits specialized TLS polymerases, which are able to synthesize over DNA lesions, thereby allowing replication of damaged templates. TLS polymerases frequently incorporate wrong nucleotides, thus resulting in the induction of mutagenesis (Sale, 2013). Interestingly, TLS-dependent mutagenesis has been observed in cells treated with FA (Grogan and Jinks-Robertson, 2012). To test a putative link between Wss1 and PRR, we investigated if FA-induced mutagenesis is affected in cells lacking Wss1. To this end, we assessed forward mutagenesis at the *CAN1* locus. *CAN1* encodes a plasma membrane arginine permease (normally used to import arginine), through which the toxic arginine analog canavanine is imported into cells. Cells with an intact *CAN1* locus are therefore highly sensitive to canavanine. Mutagenesis at the *CAN1* locus can therefore be measured by the appearance of canavanine resistant clones within a population. To measure FA-induced mutagenesis we treated cells with a short (15 min) pulse of FA (untreated cells were used as a reference) followed by plating of appropriate dilutions on either non-selective plates (to determine the total viable cell number) or plates containing canavanine (to score the frequency of canavanine resistant clones). Colonies were counted after a 3 day incubation at 30°C and mutagenesis rates were then scored as the number of canavanine resistant clones per total cell number. We could confirm TLS-dependent mutagenesis upon FA exposure, as WT cells displayed increased levels of mutagenesis when treated with increasing concentrations of FA, which was absent in cells lacking the TLS polymerase Rev3 ($\Delta rev3$) (Figure 20A). FA-induced mutagenesis was indeed affected in cells lacking Wss1, which display decreased levels of mutagenesis (Figure 20A). Notably, this effect was specific for DPCs, as mutagenesis and thus translesion synthesis was unaffected if induced by UV-light (Figure 20B). In agreement, the deletion of *REV3* does not further increase the FA sensitivity of cells lacking Wss1, even when lacking NER as well (Figure 20C).

Taken together, these results suggest that Wss1 directs repair pathway choice during DPC repair. In the absence of Wss1, cells rely more on potentially harmful recombination pathways. By contrast, if Wss1 is present translesion synthesis can occur, allowing replication of DPC-containing templates, thereby ensuring genomic stability in the face of DPCs.

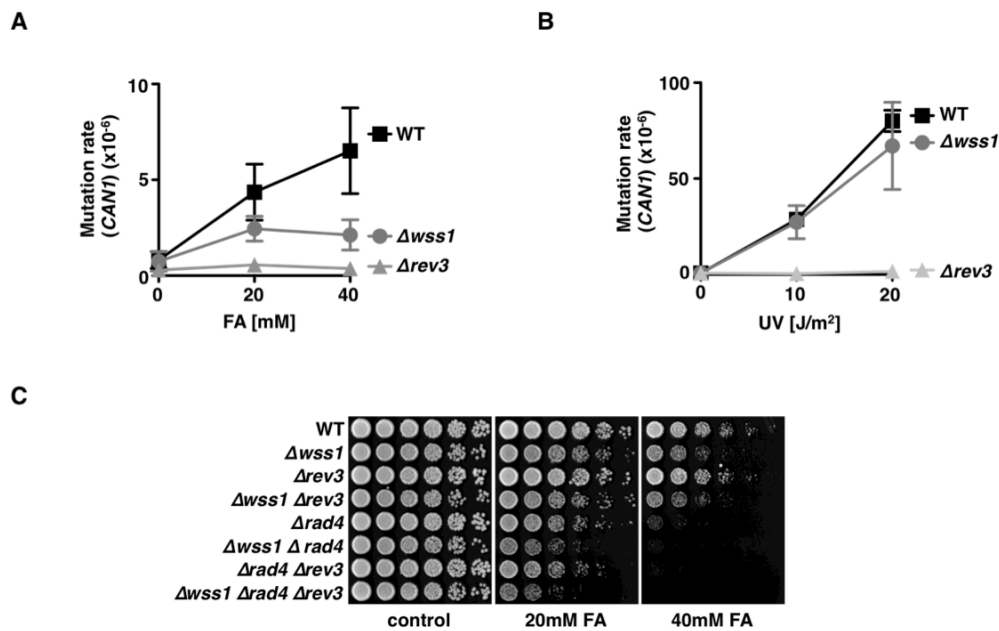


Figure 20. Wss1 promotes translesion synthesis of DPC-containing templates. (A) FA-induced mutagenesis is reduced in cells lacking Wss1. Mutagenesis was assessed at the *CAN1* locus. Cells were either untreated or subjected to a 15 min pulse treatment with the indicated FA concentration with PBS. Mutagenesis was then detected by plating cells on canavanine containing plates and determination of the number of canavanine resistant clones (only cells with a mutated non-functional *CAN1* gene are resistant to canavanine and can thus form colonies). The total viable number of cells was determined in parallel by plating appropriate dilutions on non-selective plates. Plating was performed in technical triplicates. Values represent mean values of 3 - 7 independent experiments \pm SD. **(B)** UV-induced mutagenesis is unaffected by the absence of Wss1. UV-induced mutagenesis was assessed at the *CAN1* locus. Appropriate dilutions of cells were plated on canavanine-containing plates (to determine the number of mutants) and non-selective plates (to determine the total viable cell number). Plates were then either untreated or irradiated with the indicated doses of UVC-light and then incubated in the dark for 3 d at 30°C. Mutation rates were scored as the number of canavanine resistant clones per total viable cells. Values represent mean values of 3 - 7 independent experiments \pm SD. **(C)** Deleting the gene encoding the TLS polymerase Rev3 from cells lacking Wss1 does not further increase FA sensitivity, even in cells lacking NER ($\Delta rad4$) in addition. The respective yeast strains were washed once in PBS and then incubated in PBS containing the indicated FA concentrations for 15 min under constant shaking. Following two wash steps, cells were then spotted in five-fold serial dilutions on YPD plates and incubated at 30°C for 2.5 days.

4 Discussion

This study describes a novel DNA repair mechanism dedicated to the repair of DPCs. This mechanism is built around the metalloprotease Wss1, which is the first DNA repair enzyme devoted specifically to the repair of DPCs. Importantly, Wss1 appears to have the unique ability to target all kinds of DPCs, irrespective of the identity of the involved proteins.¹

4.1 DNA-protein crosslink repair

The genetic and biochemical data presented in this study allow to propose a partially hypothetical model for the repair of DPCs (Figure 21). The repair of DPCs comprises three genetically distinct pathways: NER, HR and the pathway comprising Wss1. Nucleotide excision repair (NER) has been shown previously to confer resistance toward FA-induced DPCs (de Graaf et al., 2009). In addition, we discovered that NER is responsible for clearing the majority of DPCs, as cells lacking the NER pathway ($\Delta rad4$) display a significant delay in FA-induced DPCs. DPC clearing by NER is apparently independent of the cell cycle, as NER deficient cells do not accumulate in a specific cell cycle phase (Figure 17). This is in contrast to cells lacking either recombination or Wss1, in which initial DPC clearing appears to be functional, yet which accumulate specifically in the late S/G2 phase of the cell cycle (Figure 17). We attribute the defect seen in cells lacking Wss1 or HR to DPCs, which have escaped repair by NER prior to S-phase or are resistant to NER. This is likely the case for DPCs containing very large protein components, as it was shown *in vitro* that NER is incapable of excising large DPCs (Ide et al., 2008). DPCs, which have not been repaired prior to cells entering S-phase pose a significant threat towards cellular integrity, as they will likely stall approaching replication forks. The data presented in this study indicate that cells possess two distinct mechanisms to address the problem of DPC-stalled replication forks: DPC repair and DPC tolerance.

4.1.1 DPC repair

The DPC repair pathway is built around the DPC-processing protease (termed DPC protease in the following) Wss1 and provides resistance towards Top1- and FA-induced DPCs. The current model is that Wss1 breaks down the bulk of the protein components of DPCs proteolytically, thereby enabling progression of the replicative

¹ Parts of this Discussion will be published as a review article in *Trends in Biochemical Sciences*. Stingele et al., DNA-protein crosslink repair: proteases as DNA repair enzymes (commissioned review in preparation).

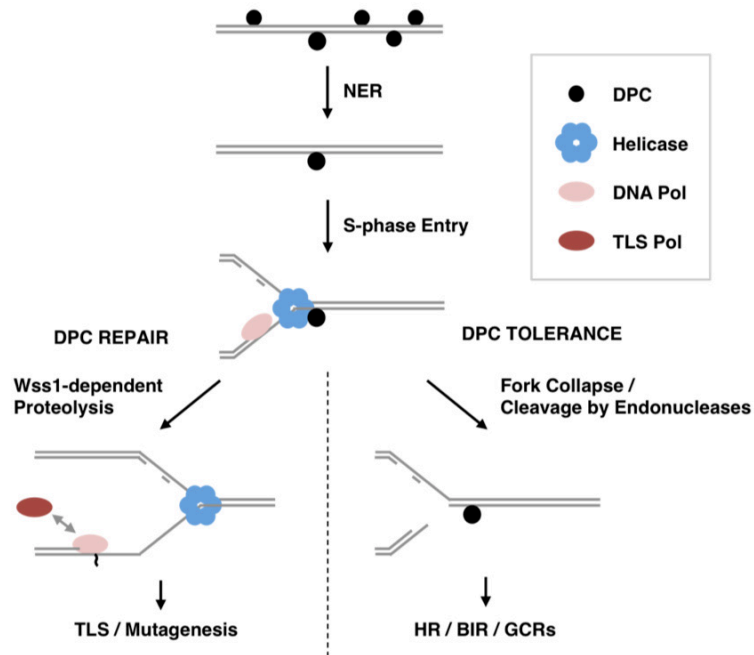


Figure 21: The bulk of DPCs are repaired by NER, but DPCs that escaped repair are expected to stall replicative helicases during S phase. Helicase stalling might be relieved by Wss1-dependent DPC processing (left). However, replicative polymerases are probably unable to replicate past the remaining lesion (proteolytic fragment remnant covalently bound to DNA), causing an uncoupling of DNA unwinding and DNA synthesis and resulting in an enlargement of single-stranded DNA. Accumulation of single-stranded DNA, in turn, promotes PCNA monoubiquitylation and subsequent recruitment of TLS polymerases. Because TLS polymerases are able to synthesize past the lesion yet potentially by misincorporation of nucleotides, mutagenesis can occur. Conversely, if a DPC is left unprocessed (right), the permanently stalled replication fork might be subjected to cleavage by endonucleases, resulting in a single-ended double-strand break. This situation may trigger recombination-dependent repair, e.g. by break-induced replication (BIR), though with the risk of genomic rearrangements (GCRs).

helicase. The remaining peptide remnant covalently bound to DNA will still block replicative polymerases. As a consequence single-stranded DNA will be formed due to the uncoupling of DNA unwinding and synthesis. Accumulated single-stranded DNA triggers PCNA ubiquitylation. This allows replication to continue by recruitment of mutagenic TLS polymerases, which are able to replicate even across bulky DNA lesions. This model is supported by the fact that formaldehyde induces mutagenesis (Grogan and Jinks-Robertson, 2012), and that this TLS-mediated reaction partially depends on Wss1 (Figure 20). However, it seems that the TLS step is of minor importance for cellular integrity, as the deletion of the TLS polymerase Rev3, which is responsible for the FA-induced mutagenesis, does not render cells sensitive toward FA (Figure 20). The small peptide remnant, which remains crosslinked to DNA, may be eventually excised by NER. The idea, that NER and Wss1 are partially acting up- and downstream of each other is supported by the fact, that the deletion of the gene

encoding Wss1 has a significantly milder effect in NER-deficient strains than in recombination deficient strains (Figure 16). Taken together, DPC repair provides resistance towards DPCs by enabling replication of DPC containing templates, however bears the risk of inducing mutagenesis.

4.1.2 DPC tolerance

In addition to DPC repair, DPC tolerance mediated by a recombination-based mechanism may allow replication of DPC-containing templates, however without actually removing the DPC. DPC tolerance likely involves the generation of single-ended DNA double-strand breaks (DSBs) either by replication fork run-off, as in the case of Top1-dependent DPCs, or endonucleolytic cleavage, as for nonenzymatic DPCs. These single-ended DSBs are subsequently repaired by break-induced replication (BIR) or homologous recombination (HR), which, however bear the risk of causing genome rearrangements. Because this alternative pathway is principally active in the absence of the DPC protease, cells lacking Wss1 suffer from hyper-recombination and genomic rearrangements (Figure 19).

4.2 Regulation of Wss1

In vitro, Wss1 has the astonishing ability to cleave any protein (tested so far), as long as it is bound to DNA. This remarkable promiscuity is, of course, ideal for an enzyme targeting nonenzymatic DPCs, which can, at least theoretically, involve almost any protein. However, Wss1's ability to cleave any DNA-bound protein is a potentially very toxic activity. Generally, cells use sophisticated strategies to restrain uncontrolled proteolytic cleavage, which includes the expression of proteases as inactive precursors (zymogens), spatial sequestration (lysosomal proteases), confined active sites (proteasome) or active sites with high sequence specificity. An important regulatory mean to minimize unwanted cleavage, is perhaps the cellular concentration of Wss1, which is expressed at extremely low levels. In addition, Wss1's ability to cleave another protein *in vitro* is entirely dependent on DNA in order to bring substrate and enzyme together. If this is also the case *in vivo* is currently not testable, as it has not been successful so far to generate Wss1 variants unable to bind DNA. These variants, when tested in complementation assays, would reveal if DNA binding is also required *in vivo*. Furthermore, the requirements for DNA *in vitro* do not appear to be very strict, but DNA *in vivo* is mostly chromatinized and, thus, might be insulated against Wss1 activation. Notably, chromatin undergoes intensive remodeling at sites of DNA damage and repair, which may open up the possibility for Wss1 activation (Tsabar and Haber, 2013). However, the exact mechanisms for controlling Wss1's activity remain elusive at the moment, but it is likely that SUMO and Cdc48 are involved, given that SUMO and Cdc48 are critically important for Wss1's role *in vivo*.

4.2.1 Wss1 and SUMO

Wss1's functions seems to be linked to the SUMO-system, as SUMO-binding is partially required for its function *in vivo* (Figure 9). The observation that Wss1 variants lacking SUMO-binding capacity retain a certain degree of functionality might be explained by the fact that Wss1's binding partner Cdc48 bears SUMO binding properties itself (Bergink et al., 2013). Thus, the Wss1-Cdc48 complex likely remains able to bind SUMO, even if crucial residues in Wss1's SIMs are altered. Nonetheless, the exact function of SUMO binding by Wss1 remains unclear and deserves further attention. Protein modification by SUMO is a well-known targeting factor, especially in DNA repair pathways. SUMOylation targets proteins to specific sites via two distinct mechanisms (Jentsch and Psakhye, 2013). (1) Selective SUMOylation

targets specific substrates, which are then recognized by SIMs of their binding partner. As the binding partners often possess, in addition to the SIM, direct recognition motifs for the SUMOylated substrates, a high degree of specificity is achieved. For instance, the anti-recombinase Srs2 is recruited to SUMOylated PCNA by a SIM and a PIP-box, which binds PCNA directly (Pfander et al., 2005). Alternatively, (2) SUMOylation can target entire groups of proteins, such as those required for HR-dependent repair of DSBs (Psakhye and Jentsch, 2012). In these cases, SUMO is proposed to act as glue tethering protein assemblies together in order to facilitate complex molecular processes, such as those occurring during HR. Both scenarios, substrate selective or protein group SUMOylation, are conceivable for targeting Wss1. The DPC itself might be SUMOylated to mark it for cleavage by Wss1. Support for this idea, comes from the observation that Top1 becomes extensively SUMOylated upon exposure to CPT, i.e. upon covalent trapping on DNA (Chen et al., 2007b; Mao et al., 2000). Another possibility is, that the entire stalled replisome along with the DPC undergo group SUMOylation, which then in turn facilitates Wss1 recruitment.

4.2.2 Wss1 and Cdc48

Cdc48-binding is absolutely required for Wss1's function *in vivo* (Figure 8), but it is currently not clear what Cdc48 actually contributes to the repair of DPCs. The segregase Cdc48 is well known for its function in segregating proteins from their environment (Jentsch and Rumpf, 2007). In recent years it became increasingly apparent that Cdc48 is commonly required to extract proteins from chromatin (Dantuma and Hoppe, 2012). Therefore, it seems reasonable to speculate that Cdc48 may be required to extract DPC fragments generated by Wss1-dependent proteolysis. The proteins involved in DPCs are most likely DNA-binding proteins, which are generally very positively charged. Consequently, fragments resulting from a cleaved DPC are probably positively charged as well and are, thus, prone to remain unspecifically associated with the DNA and may therefore require Cdc48 for extraction. Alternatively, Cdc48 might "prepare" the DPC for cleavage by Wss1. Cdc48 has the ability to partially unfold proteins, which was shown to be important for proteasomal degradation of proteins lacking unstructured regions (Beskow et al., 2009). As a consequence, it seems possible that Cdc48 would be able to partially unfold the protein component of the DPCs, which may significantly facilitate cleavage by Wss1.

4.3 A conserved family of DPC proteases?

DPC proteases are highly advantageous for cells as they enable replication completion in the face of DPCs and thus promote genome stability. However, if similar enzymes and repair mechanisms exist in higher eukaryotes is currently unclear. We collaborated with Bianca Habermann (Computational Biology Group, MPI for Biochemistry), who conducted reciprocal BLAST searches in order to identify proteins homologous to Wss1 in other species. Proteins with high sequence similarity to *S. cerevisiae* Wss1 were readily identified in other fungi as well as in plants (Wss1 branch) (Figure 22A). In addition, plants and some other fungi have a second type of Wss1-like proteases, which however display a distinct domain organization (UBL-Wss1 branch). In metazoans, one type of proteases exists with weak, yet significant, homology to the protease domain of Wss1 (Spartan branch). The human member of this class is Spartan (also called Dvc1 or C1orf124). Notably, Spartan has already been suggested to be potentially related to Wss1 (Mosbech et al., 2012). The phylogenetic analysis now clearly identifies a common ancestry between Wss1 and Spartan proteases. In addition to the homologies within the protease domains both proteases display a strikingly similar domain organization (Figure 22B). The amino (N)-terminal protease domain is followed by carboxy (C)-terminal tails containing distinct protein-protein interaction motifs and domains. Both, Wss1 and Spartan proteases, bear sequence motifs for binding to the segregase Cdc48 (or p97 in higher eukaryotes), followed by domains at the far C-terminus required for the interaction with either ubiquitin (Spartan) or SUMO (Wss1). Notably, Spartan possesses an ubiquitin-binding zinc finger (UBZ), whereas Wss1 employs two SUMO interacting motifs (SIMs). Proteins of the Spartan family additionally possess short interaction motifs (PIP-boxes) for binding the replication clamp PCNA.

An orthologous relationship between Wss1 and Spartan and a common function in DPC repair is, next to sequence homology and similar domain organization, further suggested by functional data. Intriguingly, Spartan has been, similar to Wss1, implicated in repair processes at the replication fork. A series of recent reports described an involvement of Spartan in TLS, with its precise role however being highly controversial (Centore et al., 2012; Davis et al., 2012; Ghosal et al., 2012; Juhasz et al., 2012; Kim et al., 2013; Machida et al., 2012; Mosbech et al., 2012). For instance, some groups report that Spartan recruitment to stalled forks depends on Rad18-dependent PCNA ubiquitylation (Centore et al., 2012; Ghosal et al., 2012; Juhasz et al., 2012; Machida et al., 2012), whereas others report it to be

Despite these conflicting reports, it is evident that Spartan shares several functional characteristics with Wss1 (Figure 22C). Both proteases bind the segregase Cdc48 (p97 in mammals) and the interaction is essential for their function *in vivo* (Ghosal et al., 2012) (this study). Moreover, Spartan and Wss1 are both targeted to DNA either via direct DNA-binding (Wss1) or through interaction with the DNA-binding protein PCNA (Spartan) (this study) (Centore et al., 2012). If Spartan is also able to bind DNA directly has not been tested so far. In addition, targeting of both proteases involves binding to either ubiquitin (Spartan) or SUMO (Wss1). Spartan variants deficient for ubiquitin binding fail to localize to sites of DNA damage and are not able to complement Spartan deficiency (Centore et al., 2012). Similarly, Wss1 variants lacking SUMO binding fail to fully complement the loss of Wss1 (this study). However, the identity of the modified protein(s) is currently either unknown (Wss1) or under debate (Spartan). Next to regulated targeting, Spartan and Wss1 are controlled via their protein levels. Wss1, which is already expressed at extremely low levels, undergoes self-cleavage *in trans* (i.e. one Wss1 molecule cleaves another one) *in vitro* and *in vivo*. Spartan levels are regulated by proteasomal degradation mediated by the cell cycle-specific E3-Ligase APC-Cdh1 (Mosbech et al., 2012). This results in Spartan being present only in the S/G2 phase of the cell cycle. As discussed above, the tight regulation of these proteases can be explained by the fact that intracellular proteases are potentially very toxic. Whether Spartan's protease activity is also DNA-dependent is currently unclear. Generally, the requirement of Spartan's protease activity for its cellular function has only been addressed sparsely. The only report investigating Spartan's catalytic activity so far revealed, that at least for the suppression of mutagenesis its activity is required (Kim et al., 2013). Most other recent articles described Spartan rather as a scaffold, which acts nonenzymatically, yet none of these reports addressed its proteolytic activity at all (Centore et al., 2012; Davis et al., 2012; Ghosal et al., 2012; Juhasz et al., 2012; Mosbech et al., 2012). This, together with the discrepancies within the literature on Spartan, makes it currently impossible to infer a model for its molecular function in DNA repair. An idea how far-reaching Spartan's cellular activity is came from very recent studies on flies and human patients. In *Drosophila*, Spartan deficiency results in a failure to replicate specifically paternal DNA during the first mitosis of the zygote (Delabaere et al., 2014). Because paternal DNA is densely packaged in sperm involving histone-to-protamine transitions, the authors speculate that this reaction might cause DNA damage, perhaps DPC formation, requiring Spartan for repair. Furthermore,

mutations in Spartan were identified to cause early onset hepatocellular carcinoma (HCC), genomic instability and progeroid features in human patients (Lessel et al., 2014). All three known patients developed HCC in their young adulthood, which is especially intriguing as this is the place in the human body, where most reactive substances are produced.

To sum up, further efforts are needed, to clarify Spartan's role not only in TLS but, importantly, also in DPC repair, as we believe, that Spartan is the prime candidate for a Wss1-like DPC protease in higher eukaryotes for three reasons: (1) sequence homology, (2) domain organization and (3) functional analogies.

5 Materials and Methods

Unless stated otherwise chemicals and reagents were purchased from Applied Biosystems, BD, Biomol, Bio-Rad, Enzo, GE Healthcare, Life, Merck, Millipore, New England Biolabs, Peqlab, Pierce, Promega, Roche, Roth, Serva, Sigma and Thermo Scientific. Sterile flasks, sterile and de-ionized water as well sterile solutions were used in all experiments described. Microbiological, molecular biological and biochemical methods described below are based on standard procedures or on the instructions provided by the manufacturer (Ausubel, 2010; Sambrook, 2001).

5.1 Microbiological techniques

5.1.1 *Escherichia coli* (*E. coli*) techniques

E. coli strains

Strain	Genotype	Source
XL-1 Blue	<i>recA1 endA1 gyrA96 thi-1 hsdR17 supE44 relA1 lac</i> [F' <i>proAB lacIqZΔM15 Tn10</i> (Tetr)]	Stratagene
Rosetta	F ⁻ <i>ompT hsdS_B(r_B⁻ m_B⁻) gal dcm</i> pRARE (Cam ^R)	Millipore
M15 pREP4	<i>Nals, Strs⁻, Rifs⁻, Thi⁻, Lac⁻, Ara⁺, Gal⁺, Mtl⁻, F⁻, RecA⁻, Uvr⁺, Lon⁺</i>	Qiagen

E. coli media

LB medium/plates	1 % Tryptone 0.5 % yeast extract 1 % NaCl 1.5 % agar - only for plates sterilized by autoclaving
------------------	--

If applicable, antibiotics were added for plasmid selection (100 µg/ml ampicillin, 30 µg/ml kanamycin and/or 34 µg/ml chloramphenicol).

E. coli vectors

Vector	Purpose	Source
<i>pQE32</i>	Expression of His-tagged proteins	Qiagen
<i>pGEX4T1</i>	Expression of GST-tagged proteins	GE
<i>pCoofy10</i>	Expression of untagged proteins	MPIB core facility

***E. coli* plasmids**

Name	Plasmid	References
D1205	<i>pQE32-Cdc48</i>	Jentsch collection
D2102	<i>pQE32-Smt3</i>	Jentsch collection
D4269	<i>pCoofy10-Wss1</i>	PhD thesis M. Schwarz
D4270	<i>pCoofy10-wss1^{EQ}</i>	this study
D4271	<i>pCoofy10-wss1^{SHP/VIMmut}</i>	this study
D4272	<i>pCoofy10-wss1^{SIM1/2mut}</i>	this study
D4273	<i>pGEX4T1-wss1^{aa148-C}</i>	this study
D4274	<i>pGEX4T1-wss1^{aa148-C_SIM1mut}</i>	this study
D4275	<i>pGEX4T1-wss1^{aa148-C_SIM2mut}</i>	this study
D4276	<i>pGEX4T1-wss1^{aa148-C_SIM1/2mut}</i>	this study
D4277	<i>pGEX4T1-wss1^{aa148-C_SHPmut}</i>	this study
D4278	<i>pGEX4T1-wss1^{aa148-C_VIMmut}</i>	this study
D4279	<i>pGEX4T1-Wss1^{aa148-C_SHP/VIMmut}</i>	this study
D4280	<i>pGEX4T1-Ubi-Smt3-V5</i>	this study
D4281	<i>pGEX4T1-wss1^{aa148-247}</i>	this study
D4282	<i>pGEX4T1-wss1^{aa148-208}</i>	this study
D4283	<i>pGEX4T1-wss1^{aa148-181}</i>	this study
D4284	<i>pGEX4T1-wss1^{aa161-208}</i>	this study
D4285	<i>pGEX4T1-wss1^{aa181-208}</i>	this study

Preparation of competent *E. coli* cells

Plasmid DNA was transformed into *E. coli* cells using chemical transformation. Chemical-competent *E. coli* cells were generated using the following protocol. LB media was inoculated with an OD₆₀₀ of 0.05 from an overnight culture (grown at 37°C and inoculated from a single colony). The culture was grown at 37°C until it reached an OD₆₀₀ of 0.5. The culture was then cooled on ice for 15 min (from now on only cooled containers and solutions were used) and cells were harvested by centrifugation (4000 g, 15 min). Cells were resuspended in cold Tfb1 buffer (30 ml buffer per 100 ml culture, Tfb1 buffer recipe: 30 mM KAc, 50 mM MnCl₂, 100 mM KCl, 15 % glycerol, pH 5.8 (adjusted with HAc)). After 15 min on ice, cells were again harvested by centrifugation and carefully resuspended in Tfb2 buffer (5 ml buffer per 100 ml culture, Tfb2 buffer recipe: 10 mM MOPS, 7.5 mM CaCl₂, 10 mM KCl, 15 % glycerol, pH 7 (adjusted with NaOH)). Cells were aliquoted after a 5 min incubation on ice, frozen in liquid nitrogen and stored at -80°C.

Transformation of *E. coli* cells

Chemical-competent *E. coli* cells were transformed with plasmid DNA using the following protocol. Competent cells were thawed on ice directly before use. 20 - 50 μ l cells were mixed with plasmid DNA (10 ng) or ligation products (half reaction) and incubated on ice for 15 min, followed by a heat shock at 42°C for 45 sec. After cooling on ice, cells were recovered in 1 ml pre-warmed LB media for 1 hr on a rotating shaker and subsequently plated on LB plates containing the respective antibiotics.

Expression of recombinant proteins in *E. coli*

Wss1

Wss1 and variants were expressed in Rosetta cells. Expression was induced with 1 mM IPTG in a 1 l fermenter (Labfors, Infors HT) for 3 hrs at 30°C. Biomass was harvested by centrifugation and stored at -80°C.

GST-tagged proteins

GST-tagged C-terminal tails of Wss1 and GST-Ubi-Smt3-V5 were expressed in Rosetta cells. Liquid cultures were inoculated from an overnight culture with an OD₆₀₀ of 0.1 and grown at 30°C until OD₆₀₀ reached 0.4. Cultures were then shifted to RT and incubated for 1hr, prior to induction of expression with 1 mM IPTG. Expression was performed overnight and was followed by cell harvest and storage at -80°C.

His-tagged proteins

His-tagged Smt3 and Cdc48 were expressed in M15(pREP4) cells. Expression was performed essentially as for GST-tagged proteins. Importantly, His-tagged Cdc48 was immediately purified after expression, as freezing of the cell pellet resulted in very poor yields.

5.1.2 *Saccharomyces cerevisiae* (*S. cerevisiae*) techniques

S. cerevisiae strains

Strain	Genotype	References
DF5	<i>trp1-1(am) ura3-52 his3Δ200 leu2-3,11 lys2-801,</i>	(Ulrich and Jentsch, 2000)
Y0649	DF5, <i>cdc48-6</i>	(Bergink et al., 2013)
Y0710	DF5, <i>his1-1/his1-7</i>	(Pfander et al., 2005)
Y0933	RC757 Mat alpha, <i>his6 met1 sst2-1 cyh2 can1</i>	Jentsch yeast coll.
Y0934	RH448 Mat a, <i>leu2 his4 lys2 ura3 bar1</i>	Jentsch yeast coll.
YJS23	DF5, <i>rev3::hphNT1</i>	This study
YJS26	DF5, <i>rev3::hphNT1 wss1::natNT2</i>	This study
YJS87	DF5, <i>wss1::natNT2</i>	This study
YJS159	DF5, <i>tdp1::kanMX6</i>	This study
YJS251	DF5, <i>his1-1/his1-7 wss1::kanMX6/wss1::hphNT1</i>	This study
YJS255	DF5, <i>rad4::hphNT1</i>	This study
YJS257	DF5, <i>wss1::natNT2 rad4::hphNT1</i>	This study
YJS273	DF5, <i>pADH-3HA-TOP1 wss1::natNT2 tdp1::kanMX6</i>	This study
YJS324	DF5, <i>rad4::hphNT1 rev3::klTRP1</i>	This study
YJS325	DF5, <i>wss1::natNT2 rad4::hphNT1 rev3::klTRP1</i>	This study
YJS326	DF5, <i>rad4::hphNT1 rad52::URA3</i>	This study
YJS327	DF5, <i>wss1::natNT2 rad4::hphNT1 rad52::URA3</i>	This study
YJS329	DF5, <i>rad52::URA3</i>	This study
YJS330	DF5, <i>wss1::natNT2 rad52::URA3</i>	This study

YJS385	DF5, <i>wss1::natNT2 tdp1::kanMX6 rad9::hphNT1</i>	This study
YNB3	DF5, <i>can1::hphNT1 CAN1-URA3::ChrXV</i>	with N. Blömeke
YNB4	DF5, <i>can1::hphNT1 CAN1-URA3::ChrXV wss1::natNT2</i>	with N. Blömeke
YNB24	DF5, <i>can1::hphNT1 CAN1-URA3::ChrXV top1::His3MX6 wss1::natNT2</i>	with N. Blömeke
YNB25	DF5, <i>can1::hphNT1 CAN1-URA3::ChrXV top1::His3MX6</i>	with N. Blömeke
YMIS7	DF5, <i>wss1::natNT2 cdc48-6</i>	PhD thesis M. Schwarz
YMIS13	DF5, <i>wss1::natNT2 tdp1::kanMX6</i>	PhD thesis M. Schwarz
YMIS49	DF5, <i>tdp1::natNT2 cdc48-6</i>	PhD thesis M. Schwarz
YMIS103	DF5, <i>wss1::natNT2 tdp1::kanMX6 top1::His3MX6</i>	PhD thesis M. Schwarz
YMIS694	DF5, <i>pADH-3HA-TOP1</i>	PhD thesis M. Schwarz
YMIS706	DF5, <i>TOP1-3HA:: hphNT1 wss1::natNT2</i>	PhD thesis M. Schwarz
YMIS736	DF5, <i>pADH-3HA-TOP1 wss1::natNT2</i>	PhD thesis M. Schwarz
YMIS740	DF5, <i>pADH-3HA-TOP1 tdp1::kanMX6</i>	PhD thesis M. Schwarz

***S. cerevisiae* vectors**

Vector	Purpose	Source
<i>p415pADH</i>	Expression of genes under control of the <i>ADH</i> promoter	(Mumberg et al., 1995)
<i>p415pWSS1</i>	Expression of genes under control of the <i>WSS1</i> promoter	this study

***S. cerevisiae* plasmids**

Name	Plasmid	References
V0053	<i>p415-pADH</i>	(Mumberg et al., 1995)
D4260	<i>p415-pWSS1</i>	this study
D4253	<i>p415-pADH-3HA-WSS1</i>	this study
D4254	<i>p415-pADH-3HA-wss1^{EQ}</i>	this study
D4261	<i>p415-pWSS1-3HA-WSS1</i>	this study
D4262	<i>p415-pWSS1-3HA-wss1^{EQ}</i>	this study
D4263	<i>p415-pWSS1-3HA-wss1^{SHPmut}</i>	this study
D4264	<i>p415-pWSS1-3HA-wss1^{VIMmut}</i>	this study
D4265	<i>p415-pWSS1-3HA-wss1^{SHP/VIMmut}</i>	this study

D4266	<i>p415-pWSS1-3HA-wss1^{SIM1mut}</i>	this study
D4267	<i>p415-pWSS1-3HA-wss1^{SIM2mut}</i>	this study
D4268	<i>p415-pWSS1-3HA-wss1^{SIM1/2mut}</i>	this study

***S. cerevisiae* media**

YPD medium/plates	1 % yeast extract 2 % bacto-peptone 2 % glucose 2 % agar - only for plates sterilized by autoclaving
YPD G418/NAT/Hph plates	after autoclaving YPD media containing 2 % agar was cooled to 50°C prior to adding the respective antibiotic (200 mg/l G418 (geneticine, PAA laboratories), 100 mg/l NAT (nourseothricin, HK Jena), 500 mg/l Hph (hygromycin B, PAA laboratories))
SC medium/plates	0.67 % yeast extract 0.2 % amino acid drop-out mix (one or more amino acids may be omitted to select for auxotrophy markers) 2 % glucose 2 % agar - only for plates sterilized by autoclaving
Amino acid drop-out mix	20 mg Ade, Ura, Trp, His 30 mg Arg, Tyr, Leu, Lys 50 mg Phe 100 mg Glu, Asp 150 mg Val 200 mg Thr 400 mg Ser
Sporulation medium	2 % KAc, sterilized by autoclaving

Cultivation and storage of *S. cerevisiae*

Yeast cells were either cultivated on agar plates or in liquid cultures at 30°C, if not indicated otherwise. For cultivation on agar plates yeast cells were streaked with a sterile toothpick or glass pipette. Liquid cultures were typically inoculated from overnight cultures (5 - 25 ml, inoculated from a single yeast colony on an agar plate) with

an OD₆₀₀ of 0.2. Cultures were then grown until mid-log phase (OD₆₀₀ = 0.5 - 1.0) under constant shaking (150 - 250 rpm on a shaking platform). Optical density was determined photometrically with an OD₆₀₀ of 1.0 assumed to correspond to 1.5 x 10⁷ cells. Agar plates were sealed with parafilm and placed for short-term storage at 4°C. For long-term storage stationary cultures were mixed with 0.5 volumes of 50 % glycerol and kept at -80°C.

Notably, it was impossible to store the extreme sick *Δwss1 Δtdp1* strain as even a single restreak resulted in the acquisition of suppressing mutations. Therefore, all cultures of this strain were inoculated from freshly dissected tetrads.

Preparation of competent *S. cerevisiae* cells

Competent *S. cerevisiae* cells were generated from a 50 ml YPD culture grown to mid-log phase. Cells were harvested by centrifugation (500 g, 5 min, RT), washed with 25 ml sterile water and then with 5 ml SORB buffer (100 mM LiOAc, 10 mM Tris/HCl pH 8.0, 1 mM EDTA, pH 8.0, 1 M sorbitol, sterilized by filtration). After resuspension in 360 μl SORB buffer 40 μl carrier DNA (hering sperm DNA, Invitrogen, heat-denatured at 95°C for 10 min) was added and cells were either used directly for transformation or stored in aliquots at -80°C.

Transformation of *S. cerevisiae* cells

For transformation of *S. cerevisiae* competent cells were mixed with DNA (for plasmid trafo 19 μl cells + 1 μl DNA ("Mini-prep"), for integration 50 μl cells + 10 μl PCR product). 6 volumes of PEG buffer (100 mM LiOAc, 10 mM Tris/HCl, pH 8.0, 1 mM EDTA, pH 8.0, 40 % PEG-3350, sterilized by filtration) were added to the DNA-cell mixture, which was then incubated at RT for 15 - 30 min prior to an heat-shock of 7.5 min (less for very temperature sensitive strains) at 42°C. Cells were then harvested by centrifugation and recovered in warm YPD media for 4 hrs prior to plating on selective plates (the recovery step was omitted for auxotrophy markers). Selection was carried out for 2-3 days at 30°C (less for temperature sensitive strains).

Genetic manipulation of *S. cerevisiae*

Genes were deleted and replaced by a selection cassette using a PCR based strategy (Janke et al., 2004; Knop et al., 1999). In brief, selection cassettes were amplified using gene specific overhangs, which led to an integration of the selection cassette at the targeted locus after transformation thereby replacing the endogenous

gene. Integration events were first selected by plating on selective media and were subsequently confirmed by colony PCR.

Mating type analysis of haploid yeast cells

The mating type tester strains RC757 (Mat alpha) and RH448 (Mat a) were used to analyze the mating type of haploid yeast cells. The tester strains are hypersensitive towards the pheromone secreted by cells of the opposing mating type. One colony of each tester strain was resuspended in 200 μ l sterile water. This solution was mixed with 50 ml 1% molten agar (dissolved in water, precooled to 44°C), which was then poured as top-agar on pre-warmed YPD plates (approx. 5 ml per plate). Strains with unknown mating type were now streaked or replica-plated on these tester plates. Strains with the opposing mating type do not allow growth of the hypersensitive tester strains, resulting in a halo (a region without growth) around the streaked strain.

Mating, sporulation and tetrad analysis

Freshly streaked strains with different mating types were mixed in 100 μ l water and spotted on warm YPD plates. Plates were incubated for at least 3 hrs at 30°C to allow mating. Subsequently cells were streaked on plates selecting for diploid cells. Diploid cells were sporulated by washing cells from an overnight culture four times in sterile water and two times with sporulation media prior to resuspension in 10 volumes sporulation media and incubation on a rotating shaker for at least 3 days at 25°C.

For tetrad dissection sporulated diploid cells were mixed 1:1 with zymolase 100T solution (1 mg/ml) and incubated for 7 min at RT. Tetrads were then dissected using micromanipulator (Singer MSM Systems) on YPD plates and incubated for 2-3 days. Subsequently genotype and mating type of each spore was determined by replica-plating on selective plates and mating type tester plates.

Growth and cell survival assays (spotting assay)

Cells from fresh overnight cultures were adjusted to an OD₆₀₀ of 1.0 in sterile water and five-fold serial dilutions were prepared in 96-multiwell plates using a multichannel pipette. The dilutions were then spotted on plates and typically incubated for 2.5 days at 30°C. For analysis of CPT sensitivity it was crucial that plates contained 1% DMSO and that the media was adjusted to pH 7.5. FA sensitivity was tested by washing 1 OD cells in 1 ml PBS prior to resuspension in 1 ml PBS containing the respective FA concentration (FA was added to PBS immediately before needed) and

incubation for 15 min on a rotating shaker. Cells were then washed twice with 1 ml PBS prior to serial dilution and plating as described above.

Preparation of denatured protein extracts (TCA precipitation)

Cells (1 OD) were harvested from exponentially grown cultures by centrifugation and immediately frozen in liquid nitrogen to extract proteins for analysis by immunoblotting. After thawing, cells were lysed by resuspension in 150 μ l 1.85 M NaOH, 7.5% β -ME and incubated for 15 min on ice. Proteins were now precipitated from the lysate by addition of 150 μ l ice-cold 55% TCA. Lysates were kept on ice for another 15 min to allow complete precipitation prior to centrifugation (10000g) for 20 min at 4°C. Finally the protein precipitate was resuspended in 2x Lämmli buffer and incubated for 5 min at 95°C.

Preparation of native whole cell extracts

Cell extracts used for inducing self-cleavage of Wss1 were prepared from yeast overnight cultures. To this end, cells (25 OD) were harvested by centrifugation, resuspended in 1 ml lysis buffer (50 mM Tris/HCl pH 7.5, 150 mM NaCl, 0.1% Triton-X100, EDTA free complete cocktail (Roche), 1 mM DTT) and lysed by bead beating (3min, $f = 30/s$) after addition of 500 μ l silica beads. After lysis, the reaction tube was punctuated in the bottom with an injection needle, followed by centrifugation to harvest the lysate into a fresh reaction tube. Finally, the lysate was cleared by centrifugation at 4°C in a tabletop centrifuge (maximum speed) and adjusted to a protein concentration of 0.75 mg/ml (judged by BioRad protein assay) with lysis buffer.

Measurement of interchromosomal recombination rates

Interchromosomal recombination rates were measured in diploid cells between the heteroalleles *his1-1* and *his1-7* by fluctuation analysis (Pfander et al., 2005). To reduce the required hands-on time a robot-assisted protocol was established. 8 parallel cultures per strain (2 ml, YPD pH 7.5) were inoculated and incubated under constant shaking over night at 30°C. Cultures were serially diluted (total dilution factor 1:20000) using a MICROLAB STAR line liquid handling workstation (Hamilton). After dilution cultures (YPD or YPD + 1 mM FA, 2ml) were incubated for 3 days (30°C, constant shaking). Appropriate dilutions of each culture (performed with the liquid handling workstation) were plated on SC plates (to determine the total viable cell number) and on SC-HIS plates (to determine the number of mutants within the culture). Plates were incubated for 3 days at 30°C prior to colony counting. Finally

recombination rates (the likelihood of one recombination event per cell division) was calculated using the FALCOR web tool (Hall et al., 2009).

Measurement of gross chromosomal rearrangement rates

GCR rates were determined using fluctuation analysis. The used GCR tester strains are constructed as reported previously (Kanellis et al., 2007). Analogous to recombination assays a robot-assisted protocol was used (Bachelor thesis N. Blömeke). 8 cultures per strain (2ml YPD, pH 7.5) were inoculated from single colonies and grown overnight under constant shaking. A liquid handling workstation was used the next day to serially dilute (total dilution factor 1:20000, final culture) the cultures. The diluted cultures (2ml, YPD or YPD + 1 mM FA) were then again incubated at 30°C for 3 days. This incubation was followed by plating appropriate dilutions of each culture (performed with the liquid handling workstation) on either SC-plates (to determine the total viable cell number) or SC-ARG plates containing canavanine and 5'FOA (to determine the number of cells lacking the left arm of chromosome XV). Plates were incubated for 3 days at 30°C prior to colony counting. Finally GCR rates (the likelihood of one GCR event per cell division) was calculated using the FALCOR web tool (Hall et al., 2009).

Measurement of mutagenesis rates

Mutagenesis rates were assessed at the *CAN1* locus. Cells (10 OD) from overnight cultures were harvested by centrifugation washed once in PBS (1 ml) and treated with 1 ml FA solution (in PBS, dilutions were prepared immediately before used) for 15 min. After two washing steps cells were serially diluted (10 fold steps) in 96-well plates. Appropriate dilutions were plated in triplicates on either SC-plates (to determine the total viable cell number) or on SC-ARG plates containing canavanine (to determine the number of cells with a mutated *CAN1* locus). Plates were incubated for 3 days at 30°C prior to colony counting. Finally, mutation rates were scored as the number of canavanine resistant clones per total viable cell number.

Cell cycle analysis by flow cytometry

To analyze cell cycle distribution cells (0.5 - 2 OD) were harvested from cultures by centrifugation and immediately fixed in 1 ml cold 70% ethanol, 50 mM Tris/HCl pH 7.8 and stored at 4°C until all samples were collected. Cells were then washed once in 1 ml Tris buffer (50 mM Tris/HCl pH 7.8) followed by RNA digestion by addition of 520 μ l RNAase solution (500 μ l Tris buffer + 20 μ l RNAase (10 mg/ml in 10 mM Tris/HCl pH 7.5, 10 mM MgCl₂, DNase activity was removed by boiling for 10 min)).

After an incubation for 4 hrs at 37°C cells were harvested by centrifugation followed by aspiration of the supernatant and resuspension in 220 μ l proteinase K solution (200 μ l Tris buffer + 20 μ l Proteinase K (10mg/ml in 50% glycerol, 10 mM Tris/HCl pH 7.5, 25 mM CaCl₂)). After an incubation at 50°C for 30 min cells were again centrifuged, followed by aspiration of the supernatant and resuspension in 500 μ l Tris buffer. After sonification of all samples (5 s, 50% cycle, minimum power, Bandelin SONOPLUS), 25 μ l of each sample was added to 500 μ l SYTOX solution (999 μ l Tris buffer + 1 μ l SYTOX green, Life Technologies). Finally fluorescence of SYTOX stained cells were detected in the FL1 of a FACSCalibur flow cytometer (Becton Dickinson).

Quantification of Top1ccs (ICE assay)

Top1ccs were measured using an ICE assay. The protocol used was adapted from previously published methods for mammalian and *S. pombe* cells (Hartsuiker et al., 2009; Subramanian et al., 2001). Cells expressing HA-tagged Top1 (200 OD) were harvested from exponentially growing cultures by centrifugation (4°C), resuspended in 25 ml cold PBS, pelleted again, resuspended in 2 ml cold PBS, transferred to a 2 ml reaction tube, pelleted again and finally frozen in liquid nitrogen. After addition of 1 ml lysis buffer (6 M guanidine chloride, 30 mM Tris/HCl pH 7.5, 10 mM EDTA, 1% sarkosyl, 1 mg/ml Pefabloc SC, EDTA free complete cocktail (Roche)), reaction tubes were filled up with zirconia beads and cell were lysed by bead beating (15 min, f = 30/s). After lysis, the reaction tube was punctuated in the bottom with an injection needle, followed by centrifugation to harvest the lysate into a reaction tube (15 ml). Lysates were incubated at 60°C for 30 min in order to strip all non-covalent bound proteins from DNA. Finally the lysate was cleared by centrifugation for 10 min and loaded onto CsCl gradients. CsCl gradients were prepared as described before (Subramanian et al., 2001). Gradients were centrifuged in a SW 41 Ti rotor (Beckman-Coulter) for 18 hrs (32000 rpm, 25°C) prior to fractionation using a liquid handling workstation. To identify DNA-containing fractions, 30 μ l of each fraction was mixed with 270 μ l SYBR gold nucleic acid stain (Life technologies) and fluorescence was recorded using an Infinite M1000 Pro microplate reader (Tecan). Fractions containing the “DNA-peak” (typically three) were pooled and concentrated using Vivaspin 2 concentrator devices (cutoff 20 kDa, vivaproducts). Buffer was exchanged to TE (10 mM Tris/HCl pH 8, 1 mM EDTA) and samples concentrated to a volume of 150 μ l. DNA content was now analyzed by agarose gel electrophoresis (0.6% gel) and staining with ethidium bromide. To analyze the amount of Top1 samples were

treated with micrococcal nuclease (15 μ l sample, 1.8 μ l micrococcal nuclease buffer (NEB), 1 μ l micrococcal nuclease (NEB)) for 20 min on ice prior to addition of 2x Lämmli buffer and analysis by SDS-PAGE followed by immuno-blotting using HA-specific antibodies.

Quantification of FA-induced DPCs

The SDS/KCl method to measure repair of DPCs was adapted with some modifications from a previously published protocol (de Graaf et al., 2009). Cells (7 OD) were harvested from exponentially growing cultures (YPD), washed once in 10 ml warm PBS and again resuspended in 5 ml warm PBS. 500 μ l of cell suspension was withdrawn as control sample ("untreated"). 4.5 ml PBS containing FA was added cells were incubated on a rotating shaker for 15 min at 30°C. After two wash steps with 10 ml warm PBS, cells were resuspended in 9 ml pre-warmed YPD. 0.7 OD cells were immediately withdrawn as time point zero. Recovery was then allowed by incubating cultures and 30°C under constant shaking. Samples (0.7 OD) were again withdrawn after 2 and 4 hrs of recovery.

All samples were processed directly after collection using the following protocol. After harvesting by centrifugation, cells were washed once with 250 μ l zymolase buffer (10 mM Tris/HCl pH 8, 1 mM EDTA), followed by resuspension in 250 μ l zymolase buffer and addition of 1 μ l zymolase solution (20 mg/ml in water, freshly prepared). Cell wall digestion was performed for 20 min at 37°C on a rotating shaker, prior to cell lysis through the addition of 250 μ l 4% SDS. Samples were then immediately frozen in liquid nitrogen. After all cells had been collected at each time-point and lysed, samples were now processed simultaneously. Samples were thawed under constant shaking at 55°C for 5 min, followed by protein precipitation on ice (5 min) after the addition of 500 μ l KCl buffer (200 mM KCl, 20 mM Tris/HCl pH 7.5). After centrifugation (microcentrifuge, maximum speed, 4°C), the supernatant was removed and used for quantification of soluble DNA. The protein pellet was resuspended in 500 μ l KCl buffer at 55°C for 5 min, followed again by precipitation on ice, centrifugation and supernatant removal. This washing procedure was repeated 3 times in total. The washed protein precipitate was finally resuspended in 500 μ l proteinase K solution (0.2 mg/ml proteinase K in KCl buffer) and protein digestion was performed at 55°C for 45 min. After protein removal 10 μ l BSA solution (50 mg/ml AMBION) was added and samples were placed immediately on ice followed again by centrifugation. The supernatant contained now the protein associated DNA (insoluble DNA). RNA was removed from soluble and insoluble DNA samples by

addition of 1 μ l RNase A (10 mg/ml) to 50 μ l sample and incubation for 30 min at 37°C. Finally soluble and insoluble DNA amounts were quantified by agarose gel electrophoresis (0.7% gel) followed by staining with SYBR gold nucleic acid stain. Stained agarose gels were scanned on a Typhoon FLA 9000 imager (GE Healthcare). Band intensities were quantified using ImageJ. For quantifications the amount of DPCs was inferred from the ratio between insoluble DNA to total DNA (insoluble plus soluble DNA).

5.2 Molecular biology techniques

5.2.1 General buffers and solutions

TE buffer	10 mM Tris/HCl pH 8 1 mM EDTA
TBE buffer (5x)	90 mM Tris 90 mM boric acid 2.5 mM EDTA pH 8.0
DNA loading dye (6x)	10 mM Tris/HCl pH 7.5 0.15% orangeG 60% glycerol 60 mM EDTA

5.2.2 DNA purification and analysis

Isolation of plasmid DNA from *E. coli*

Plasmid DNA was isolated from fresh overnight cultures (5ml LB (containing the required antibiotics) inoculated from a single colony) using a commercially available kit (AccuPrep Plasmid Mini Extraction Kit, Bioneer) closely following the manufacturers instructions.

Isolation of genomic DNA from *S. cerevisiae*

Genomic DNA was purified using a commercially available kit (Master Pure Yeast DNA Purification Kit, Epicentre) following the manufacturers instruction. Colonies from a freshly streaked plate were used for extraction.

Purification of DNA fragments from agarose gels

DNA was purified from agarose gels by excising the band of interest using a sterile scalpel followed by DNA extraction using a commercially available kit (QIAquick Gel Extraction Kit, Qiagen).

Determination of DNA concentration

DNA concentrations were determined photometrically using a NanoDrop ND-1000 spectrophotometer (PeqLab). Absorbance was measured at a wavelength of 260 nm. Concentrations were then calculated assuming that a DNA concentration of 50 $\mu\text{g/ml}$ results in an OD_{260} of 1.0.

5.2.3 Polymerase chain reaction (PCR)

Amplification of DNA fragments was carried out by PCR. Oligonucleotides (primers) used in PCR reactions were manually designed and purchased from MWG Eurofins. Reactions were carried out in a Veriti thermocycler (Applied Biosystems).

Amplification of DNA fragments for molecular cloning

DNA fragments intended for molecular cloning were amplified from genomic or plasmid using PfuUltra II Hotstart polymerase (Agilent). Reactions were performed a reaction volume of 50-100 μl and

PCR reaction mix:

- 1 μl primer A (10 pM)
- 1 μl primer B (10 pM)
- 5 μl 5x PfuUltra II buffer
- 2.5 μl dNTPs (10 μM)
- 1 μl PfuUltra II HS
- 100 ng template
- filled up to 50 μl with sterile water

Reactions were carried out using a PCR program with annealing temperature adjusted to primer melting temperatures and elongations times adjusted to expected product length according to the guidelines provided by the polymerase manufacturer.

Amplification of targeting cassettes

PCR amplification of selection cassettes used for genomic integrations were carried out using published protocols (Janke et al., 2004; Knop et al., 1999).

Yeast colony PCR

Correct integration of targeting cassettes was confirmed using colony PCR. For confirming knockouts a primer pair used with one primer annealing 300-500 bp upstream of the ATG of the knocked-out gene and the other annealing in reverse direction within the targeting cassette. This way a PCR product can only be formed if the cassette has replaced the targeted gene. Colony PCR reactions were performed exactly as published previously (Janke et al., 2004; Knop et al., 1999).

5.2.4 Molecular cloning

Digestion of DNA with restriction endonucleases

Digestion of plasmid DNA or PCR products was performed using restriction enzymes (NEB) following the instructions provided by the manufacturer. Typically 2 μ g of DNA was digested in a 30-40 μ l reaction for 1-2 hrs. Restriction fragments intended for molecular cloning were typically purified by agarose gel electrophoresis.

Ligation of DNA fragments

Ligation reactions (20 μ l) were performed using T4 DNA ligase (NEB) following the manufacturers instructions. Typically the reactions contained 100 ng linearized plasmid DNA and 3-10 fold molar excess of insert and were carried out for 30 min at RT.

DNA sequencing

DNA sequencing was carried out by the MPIB microchemistry core facility using a ABI-Prism 3730 sequencer. Sequencing reactions contained 100-200 ng DNA and 5 pmol primer and were performed with the DYEnamic ET terminator cycle sequencing kit (GE Healthcare), following the instructions provided by the manufacturer.

5.3 Biochemical techniques

General buffers and solutions

2x Lämmli buffer	125 mM Tris/HCl pH 6.8 4% SDS 20% glycerol 0.01% bromophenol blue 2.5 % β -ME
MOPS buffer	50 mM MOPS 50 mM Tris base 3.5 mM SDS 1 mM EDTA
SWIFT blotting buffer	5% 20x Swift buffer (G-Bioscience) 10% Methanol
TBS-T	25 mM Tris/HCl pH 7.5 137 mM NaCl 2.6 mM KCl 0.1% Tween 20
PBS	10 mM phosphate, pH 7.4

137 mM NaCl
2.7 mM KCl

5.3.1 Gel electrophoresis and immuno-blot techniques

SDS-polyacrylamide gel electrophoresis (SDS-PAGE)

SDS-PAGE was performed using NUPAGE precast gradient gels (4-12%, Invitrogen). Electrophoresis was carried out using MOPS buffer at a voltage of 200 V for ca. 50 min. Samples for SDS-PAGE were prepared in 1x Lämmli buffer and were heated at 95°C for at least 5 min. The Precision Plus Protein All Blue Standard (Bio-Rad) was used as a molecular weight marker in order to estimate protein sizes.

Immuno-blot analysis

Proteins separated by SDS-PAGE were transferred using a wet tank system (GE Healthcare) to polyvinylidene fluoride membranes (ImmobilionP, Millipore), which had been activated by incubation in methanol (1 min). Transfer was carried out in SWIFT blotting buffer at 75 V for 1.5 hrs at 4°C. After transfer membranes were incubated with primary antibody in blocking buffer (TBS-T, 5% skimmed milk powder) overnight. After three washes with TBS-T (10 min) membranes were incubated with HRP-coupled secondary antibodies for 30 - 90 min, followed again by three wash steps with TBS-T. Chemiluminescent signals were detected after incubating the membranes with substrate solutions (ECL, ECL-Plus or ECL advanced kits, GE Healthcare) for 1 min either by exposure of the membranes to Amersham Hyperfilm ECL (GE Healthcare) or by using a luminescent image analyzer (LAS-3000, Fujifilm).

Antibodies

Polyclonal anti-Smt3 antibody was produced in the Jentsch lab and was described before (Hoege et al., 2002). Anti- HA (F-7) antibodies were purchased from Santa Cruz Biotechnology, anti-Dpm1 (A6429) and anti-BSA (A111333) from Life Technologies, anti-Hmg1 (H9537) from Sigma-Aldrich, anti-Rad53 (104232), anti-GST (19256), anti-Top1 (28432) and anti- H1 (11079) from Abcam.

5.3.2 Protein purification and interaction analysis

Purification of recombinant proteins from *E. coli*

Wss1

Wss1 was purified in collaboration with the MPIB microchemistry core facility using the following protocol. Cells were lysed in lysis buffer (50 mM Tris pH 7.5, 10 mM

CaCl₂, 30 mM NaCl) using a high-pressure homogenizer (EmulsiFlex C5, Avestin). Inclusion bodies were pelleted by centrifugation, followed by two wash steps with wash buffer (50 mM Tris pH 7.5, 10 mM CaCl₂, 30 mM NaCl, 3% Triton X-100, 1% CHAPS) and two wash steps with lysis buffer. After resuspension in lysis buffer additionally containing 5 mM DTT inclusion bodies were solubilized by addition of 4 volumes solubilisation buffer (lysis buffer, 5 mM DTT, 8 M urea) and incubation overnight on a rotating wheel (4°C). After solubilization the solution was cleared by centrifugation. Wss1 was now refolded during five dialysis steps. First Wss1 was dialyzed against dialysis buffer 1 (50 mM Tris pH 7.5, 10 mM CaCl₂, 30 mM NaCl, 20 µM ZnCl₂, 0.5 mM DTT, 4 M urea, 0.05% Tween20), followed by dialysis against dialysis buffer 2 and 3 (identical to dialysis buffer 1, yet containing 2 M, respectively 1 M, urea in addition). The two final dialysis steps were carried out against dialysis buffer 4 (50 mM Tris pH 7.5, 10 mM CaCl₂, 30 mM NaCl, 0.05 % Tween20). Finally the Wss1 preparation was cleared from insoluble material by sterile filtration and subjected to ion exchange chromatography (Source 30S column, GE Healthcare). Wss1 eluted from the column in a single peak (elution buffer: 20 mM Tris pH 7.5, approx. 400 mM NaCl). Aliquots were immediately frozen in liquid nitrogen and stored at -80°C until used.

GST-tagged proteins

GST-tagged C-terminal tails of Wss1 and GST-Ubi-Smt3-V5 were purified from *E. coli* cells using standard protocols. In brief, cells were lysed in lysis buffer (40 mM Tris/HCl pH 7.5, 150 mM NaCl, 1x PefaBloc, 5 mM DTT, Roche complete protease inhibitors) using an EmulsiFlex C5 homogenizer (Avestin). Lysates were then cleared by centrifugation at 20 krpm for 30 min at 4°C. After addition of glutathione-Sepharose beads (equilibrated in lysis buffer, GE Healthcare), supernatants were incubated at 4°C for 2.5 hrs on a rotating wheel. Initially, beads were washed three times using lysis buffer, followed by three washes with wash buffer (lysis buffer, containing 450 mM NaCl). GST-tagged proteins were eluted using elution buffer (40 mM Tris/HCl, 50 mM reduced glutathione, 5 mM DTT, pH was adjusted to 7 - 8 with NaOH). Finally, eluted proteins were dialyzed against 5 l cold PBS overnight using slide-a-lyzer dialysis cassettes (Pierce) followed by aliquotation and freezing in liquid nitrogen.

His-tagged proteins

His-tagged proteins were purified as described for GST-tagged proteins with some modifications. Next to using Ni-NTA-agarose instead of glutathione Sepharose, the following buffers were used: lysis buffer: 40 mM Tris/HCl pH 7.5, 100 mM NaCl, 5 mM MgCl₂, 20 mM imidazole, 5 mM beta-mercaptoethanol, 1x PefaBloc, Roche complete protease inhibitors; wash buffer: as lysis buffer, yet containing a total of 50 mM imidazole (adjusted with HCl to pH 7 - 8); elution buffer: as lysis buffer, yet containing a total of 250 mM imidazole (adjusted with HCl to pH 7 - 8).

Protein-protein interaction analysis by GST-pulldown assays

In order to investigate direct binding, GST-tagged proteins (or GST alone) were incubated together with their potential binding partners and 15 μ l glutathione-Sepharose beads (50% slurry in binding buffer, GE Healthcare) in a total volume of 400 - 500 μ l binding buffer (50 mM Tris/HCl pH 7.5, 250 mM NaCl, 0.5% NP40). Samples were incubated for 1 hr at 4°C prior to centrifugation in a microcentrifuge (2 min, 2 krpm, 4°C). Supernatant was removed and beads were washed three times with 500 μ l binding buffer. After the final wash, beads were resuspended in 25 μ l Laemmli buffer. Finally, samples were analyzed by SDS-PAGE followed by Coomassie blue staining and/or immunoblotting.

Protein-DNA interaction analysis by electrophoretic mobility shift assays

Electrophoretic mobility shift assays were used for investigating the DNA-binding properties of Wss1's C-terminal tail. First, for each protein several solutions with decreasing concentrations were prepared in PBS (typically ranging from 2.25 μ M to 18 μ M). 10 μ l of each protein solution was incubated together with 2 μ l fluorescently labeled double-stranded DNA oligos (1 μ M in sterile water, sequence: Alexa488-5'-TTCCGGCTGACTCATCAAGCG-3') and 8 μ l Tris/HCl buffer (25 mM, pH 7.5). Binding reactions were incubated for 20 min at 25°C prior to adding 5 μ l loading buffer (5x NOVEX Hi-density TBE loading buffer). 6 % DNA retardation gels (Life technologies) were pre-run for 30 - 60 min in 0.5x TBE before loading 12.5 μ l of each sample. Electrophoresis were performed for 15 min at 80 V, followed by 30 min at 100 V. Electrophoretic mobility shifts were then visualized using a Typhoon FLA 9000 imager (GE Healthcare).

5.3.3 Protease assays

Wss1 self-cleavage induced by cell extracts

Whole cell extracts (WCE) were prepared from 25 OD of an overnight culture of WT strains. Cells were lysed using a bead beater (MM301, Retsch GmbH) in lysis buffer (50 mM Tris/HCl pH 7.5, 150 mM NaCl, 0.1% Triton X-100, 1 mM DTT and EDTA-free complete protease inhibitor cocktail (Roche)). WCEs were adjusted to a protein concentration of 0.75 mg/ml, as measured by Bio-Rad Protein assay. Subsequently, 40 μ l WCE was mixed with 5 μ l micrococcal nuclease buffer (50 mM MgCl₂, 50 mM CaCl₂, 5 mM DTT, 1 mM EDTA) and either 5 μ l PBS or, for nucleic acid depleted lysates, 5 μ l micrococcal nuclease (30 U/ μ l, Roche). WCEs were then incubated for 20 min either on ice or at 80°C for heat inactivated WCEs. Cleavage reactions were setup using 1 μ l Wss1 (2 mg/ml in 20 mM Tris/HCl pH 7.5, 400 mM NaCl), 3 μ l WCE and 6 μ l buffer (25 mM Tris(HCl), pH 7.5) and incubated at 30°C. Reactions were stopped at the respective time-points by addition of 1 vol. 2x Laemmli buffer. Finally, cleavage was visualized using SDS-PAGE followed by Coomassie blue staining.

Wss1 self-cleavage induced by DNA

Typically, DNA-dependent self cleavage was assayed in 10 μ l reactions, containing 1 μ l Wss1 (2 mg/ml in 20 mM Tris/HCl pH 7.5, 400 mM NaCl), 1 μ l DNA, 3 μ l sterile water and 5 μ l buffer (25 mM Tris/HCl pH 7.5, 150 mM NaCl). Several types of DNAs were used for induction of cleavage: single-stranded viral DNA (Φ X174 virion, NEB); double-stranded viral DNA (Φ X174 RF I, NEB); single- and double-stranded 32 bp oligonucleotides (5'-GCAATCGAATCCAGCTGATCAAAGAATAGCAC-3'); single-stranded 16 bp oligo nucleotides (5'-GCAATCGAATCCAGCT-3'); single-stranded 8 bp oligonucleotides (5'-GCAATCGA-3'). All oligonucleotides used were synthesized by MWG Eurofins Operon.

DNA-dependent cleavage of substrates

Cleavage assays were typically performed in reactions, containing 2 μ l substrate protein (0.5 mg/ml in 16 mM HEPES pH 8, 400 mM NaCl, 20% glycerol), 1 μ l Wss1 (2 mg/ml in 20 mM Tris/HCl pH 7.5, 400 mM NaCl), 1 μ l DNA (Φ X174 virion, 1 mg/ml in TE, NEB), 7.5 μ l H₂O and 3.5 μ l 25 mM Tris pH 7.5, 150 mM NaCl. Normally, cleavage was allowed to occur at 30°C for 2 hr. Reactions were stopped by addition of 1 vol. 2x Laemmli buffer. Cleavage was monitored by SDS-PAGE, followed by either Coomassie-blue staining or western blotting using substrate-specific antibodies. Cleavage reactions containing recombinant Top1 were digested with

micrococcal nuclease (NEB) prior to loading on SDS-PAGE gels, as Top1 displays an aberrant running behavior in the presence of DNA.

Smt3-CHOP assay

SUMO-isopeptidase activity was tested using the commercial Smt3-CHOP assay kit (Lifesensors). Assays were performed using the protocol provided by the manufacturer. Fluorescence was recorded using a M1000 Pro microplate reader (Tecan).

References

Alvaro, D., *et al.* (2007). Genome-Wide Analysis of Rad52 Foci Reveals Diverse Mechanisms Impacting Recombination. *PLoS Genet.* *3*, e228.

Arana, M.E., and Kunkel, T.A. (2010). Mutator phenotypes due to DNA replication infidelity. *Seminars in cancer biology* *20*, 304-11.

Ausubel, F.M. (2010). *Current Protocols in Molecular Biology* (John Wiley & Sons).

Barker, S., *et al.* (2005). DNA-protein crosslinks: their induction, repair, and biological consequences. *Mutat. Res.* *589*, 111-35.

Bergink, S., *et al.* (2013). Role of Cdc48/p97 as a SUMO-targeted segregase curbing Rad51-Rad52 interaction. *Nat. Cell. Biol.* *15*, 526-32.

Beskow, A., *et al.* (2009). A conserved unfoldase activity for the p97 AAA-ATPase in proteasomal degradation. *Journal of molecular biology* *394*, 732-46.

Bienko, M., *et al.* (2005). Ubiquitin-binding domains in Y-family polymerases regulate translesion synthesis. *Science* *310*, 1821-4.

Biggins, S., *et al.* (2001). Genes involved in sister chromatid separation and segregation in the budding yeast *Saccharomyces cerevisiae*. *Genetics* *159*, 453-70.

Bjornsti, M.A., *et al.* (1989). Expression of human DNA topoisomerase I in yeast cells lacking yeast DNA topoisomerase I: restoration of sensitivity of the cells to the antitumor drug camptothecin. *Cancer Res.* *49*, 6318-23.

Blastyák, A. (2014). DNA replication: damage tolerance at the assembly line. *Trends in biochemical sciences* *39*, 301-304.

Boiteux, S., and Radicella, J.P. (2000). The Human *OGG1* Gene: Structure, Functions, and Its Implication in the Process of Carcinogenesis. *Archives of biochemistry and biophysics* *377*, 1-8.

Branzei, D. (2011). Ubiquitin family modifications and template switching. *FEBS letters* *585*, 2810-7.

Centore, R.C., *et al.* (2012). Spartan/C1orf124, a reader of PCNA ubiquitylation and a regulator of UV-induced DNA damage response. *Mol. Cell* *46*, 625-35.

Champoux, J.J. (2001). DNA topoisomerases: structure, function, and mechanism. *Annu Rev Biochem* *70*, 369-413.

Chapman, J.R., *et al.* (2012). Playing the end game: DNA double-strand break repair pathway choice. *Molecular cell* *47*, 497-510.

Chen, H.J., *et al.* (2007a). Characterization of DNA-protein cross-links induced by oxanine: cellular damage derived from nitric oxide and nitrous acid. *Biochemistry* *46*, 3952-65.

Chen, X.L., *et al.* (2007b). Topoisomerase I-dependent viability loss in *Saccharomyces cerevisiae* mutants defective in both SUMO conjugation and DNA repair. *Genetics* *177*, 17-30.

Chiruvella, K.K., *et al.* (2013). Repair of Double-Strand Breaks by End Joining. *Cold Spring Harb. Perspect. Biol.* *5*.

Chodosh, L.A. (2001). UV crosslinking of proteins to nucleic acids. *Current protocols in molecular biology* / edited by Frederick M. Ausubel ... [et al.] *Chapter 12*, Unit 12.5.

Chowdhury, D., *et al.* (2013). Charity begins at home: non-coding RNA functions in DNA repair. *Nat. Rev. Mol. Cell. Biol.* *14*, 181-189.

Chvalova, K., *et al.* (2007). Mechanism of the formation of DNA-protein cross-links by antitumor cisplatin. *Nucleic Acids Res.* *35*, 1812-21.

Cleaver, J.E. (1968). Defective repair replication of DNA in xeroderma pigmentosum. *Nature* *218*, 652-6.

Compe, E., and Egly, J.-M. (2012). TFIIH: when transcription met DNA repair. *Nature Reviews Molecular Cell Biology* *13*, 343-354.

Cortes Ledesma, F., *et al.* (2009). A human 5'-tyrosyl DNA phosphodiesterase that repairs topoisomerase-mediated DNA damage. *Nature* *461*, 674-8.

D'Andrea, A.D. (2008). Chapter 4 - DNA Repair Pathways and Human Cancer. In *The Molecular Basis of Cancer (Third Edition)*, J.M.M.H.A.I.W.G.B. Thompson, ed. (Philadelphia: W.B. Saunders), pp. 39-55.

D'Andrea, A.D. (2010). Susceptibility pathways in Fanconi's anemia and breast cancer. *The New England journal of medicine* *362*, 1909-19.

Dantuma, N.P., and Hoppe, T. (2012). Growing sphere of influence: Cdc48/p97 orchestrates ubiquitin-dependent extraction from chromatin. *Trends Cell Biol.* *22*, 483-91.

Davis, E.J., *et al.* (2012). DVC1 (C1orf124) recruits the p97 protein segregase to sites of DNA damage. *Nat. Struct. Mol. Biol.* *19*, 1093-100.

de Boer, J., and Hoeijmakers, J.H. (2000). Nucleotide excision repair and human syndromes. *Carcinogenesis* *21*, 453-460.

de Graaf, B., *et al.* (2009). Cellular pathways for DNA repair and damage tolerance of formaldehyde-induced DNA-protein crosslinks. *DNA repair* *8*, 1207-14.

de Oca, R.M., *et al.* (2005). Regulated interaction of the Fanconi anemia protein, FANCD2, with chromatin. *Blood* *105*, 1003-1009.

Deans, A.J., and West, S.C. (2011). DNA interstrand crosslink repair and cancer. *Nat Rev Cancer* *11*, 467-480.

Delabaere, L., *et al.* (2014). The Spartan Ortholog Maternal Haploid Is Required for Paternal Chromosome Integrity in the *Drosophila* Zygote. *Current biology* : CB.

- Desai, S.D., *et al.* (1997). Ubiquitin-dependent destruction of topoisomerase I is stimulated by the antitumor drug camptothecin. *J. Biol. Chem.* *272*, 24159-64.
- DiGiovanna, J.J., and Kraemer, K.H. (2012). Shining a light on xeroderma pigmentosum. *The Journal of investigative dermatology* *132*, 785-96.
- Fagbemi, A.F., *et al.* (2011). Regulation of endonuclease activity in human nucleotide excision repair. *DNA repair* *10*, 722-729.
- Fei, J., *et al.* (2011). Regulation of nucleotide excision repair by UV-DDB. *PLoS biology* *9*.
- Ferretti, L.P., *et al.* (2013). Controlling DNA-end resection: a new task for CDKs. *Front. Genet.* *4*, 99.
- Friedberg, E.C., *et al.* (2014). *DNA Repair, Mutagenesis, and Other Responses to DNA Damage* (New York: Cold Spring Harbor Laboratory Press).
- Furgason, J.M., and Bahassi el, M. (2013). Targeting DNA repair mechanisms in cancer. *Pharmacology & therapeutics* *137*, 298-308.
- Garaycochea, J.I., *et al.* (2012). Genotoxic consequences of endogenous aldehydes on mouse haematopoietic stem cell function. *Nature* *489*, 571-5.
- Gherezghiher, T.B., *et al.* (2013). 1,2,3,4-Diepoxybutane-induced DNA-protein cross-linking in human fibrosarcoma (HT1080) cells. *Journal of proteome research* *12*, 2151-64.
- Ghodgaonkar, M.M., *et al.* (2013). Ribonucleotides misincorporated into DNA act as strand-discrimination signals in eukaryotic mismatch repair. *Mol. Cell* *50*, 323-32.
- Ghosal, G., *et al.* (2012). Proliferating cell nuclear antigen (PCNA)-binding protein C1orf124 is a regulator of translesion synthesis. *J. Biol. Chem.* *287*, 34225-33.
- Goodarzi, A.A., *et al.* (2006). DNA - PK autophosphorylation facilitates Artemis endonuclease activity. *The EMBO journal* *25*, 3880-3889.
- Grogan, D., and Jinks-Robertson, S. (2012). Formaldehyde-induced mutagenesis in *Saccharomyces cerevisiae*: molecular properties and the roles of repair and bypass systems. *Mutat. Res.* *731*, 92-8.
- Hall, B.M., *et al.* (2009). Fluctuation analysis CalculatOR: a web tool for the determination of mutation rate using Luria-Delbruck fluctuation analysis. *Bioinformatics* *25*, 1564-5.
- Hartley, K.O., *et al.* (1995). DNA-dependent protein kinase catalytic subunit: a relative of phosphatidylinositol 3-kinase and the ataxia telangiectasia gene product. *Cell* *82*, 849-56.
- Hartsuiker, E., *et al.* (2009). Distinct requirements for the Rad32(Mre11) nuclease and Ctp1(CtIP) in the removal of covalently bound topoisomerase I and II from DNA. *Mol. Cell* *33*, 117-23.

Helleday, T., *et al.* (2008). DNA repair pathways as targets for cancer therapy. *Nat Rev Cancer* 8, 193-204.

Heyer, W.D., *et al.* (2010). Regulation of homologous recombination in eukaryotes. *Annu. Rev. Genet.* 44, 113-39.

Hincks, J.R., and Coulombe, R.A., Jr. (1989). Rapid detection of DNA-interstrand and DNA-protein cross-links in mammalian cells by gravity-flow alkaline elution. *Environmental and molecular mutagenesis* 13, 211-7.

Hoegge, C., *et al.* (2002). RAD6-dependent DNA repair is linked to modification of PCNA by ubiquitin and SUMO. *Nature* 419, 135-41.

Hoeijmakers, J.H.J. (2001). Genome maintenance mechanisms for preventing cancer. *Nature* 411, 366-374.

Ide, H., *et al.* (2008). Repair of DNA-protein crosslink damage: coordinated actions of nucleotide excision repair and homologous recombination. *Nucleic acids symposium series* (2004), 57-8.

Iyer, L.M., *et al.* (2004). Novel predicted peptidases with a potential role in the ubiquitin signaling pathway. *Cell cycle (Georgetown, Tex.)* 3, 1440-50.

Jackson, S.P., and Bartek, J. (2009). The DNA-damage response in human biology and disease. *Nature* 461, 1071-1078.

Janke, C., *et al.* (2004). A versatile toolbox for PCR-based tagging of yeast genes: new fluorescent proteins, more markers and promoter substitution cassettes. *Yeast* 21, 947-62.

Jentsch, S., and Psakhye, I. (2013). Control of nuclear activities by substrate-selective and protein-group SUMOylation. *Annu. Rev. Genet.* 47, 167-86.

Jentsch, S., and Rumpf, S. (2007). Cdc48 (p97): a "molecular gearbox" in the ubiquitin pathway? *Trends Biochem. Sci.* 32, 6-11.

Jiricny, J. (2013). Postreplicative Mismatch Repair. *Cold Spring Harb. Perspect. Biol.* 5.

Juhasz, S., *et al.* (2012). Characterization of human Spartan/C1orf124, an ubiquitin-PCNA interacting regulator of DNA damage tolerance. *Nucleic Acids Res.* 40, 10795-808.

Kanellis, P., *et al.* (2007). A Screen for Suppressors of Gross Chromosomal Rearrangements Identifies a Conserved Role for PLP in Preventing DNA Lesions. *PLoS Genet.* 3, e134.

Khanna, K.K., and Jackson, S.P. (2001). DNA double-strand breaks: signaling, repair and the cancer connection. *Nature genetics* 27, 247-254.

Kim, M.S., *et al.* (2013). Regulation of error-prone translesion synthesis by Spartan/C1orf124. *Nucleic Acids Res.* 41, 1661-8.

- Knipscheer, P., *et al.* (2009). The Fanconi anemia pathway promotes replication-dependent DNA interstrand cross-link repair. *Science* 326, 1698-701.
- Knop, M., *et al.* (1999). Epitope tagging of yeast genes using a PCR-based strategy: more tags and improved practical routines. *Yeast* 15, 963-72.
- Kooistra, S.M., and Helin, K. (2012). Molecular mechanisms and potential functions of histone demethylases. *Nat. Rev. Mol. Cell. Biol.* 13, 297-311.
- Krokan, H.E., and Bjørås, M. (2013). Base Excision Repair. *Cold Spring Harb. Perspect. Biol.* 5.
- Lambert, S., *et al.* (2005). Gross chromosomal rearrangements and elevated recombination at an inducible site-specific replication fork barrier. *Cell* 121, 689-702.
- Langevin, F., *et al.* (2011). Fancd2 counteracts the toxic effects of naturally produced aldehydes in mice. *Nature* 475, 53-8.
- Lea, D.E., and Coulson, C.A. (1949). The distribution of the numbers of mutants in bacterial populations. *Journ. of Genetics* 49, 264-285.
- Lessel, D., *et al.* (2014). Mutations in SPRTN cause early onset hepatocellular carcinoma, genomic instability and progeroid features. *Nat Genet advance online publication*.
- Levin, D.S., *et al.* (2000). Interaction between PCNA and DNA ligase I is critical for joining of Okazaki fragments and long-patch base-excision repair. *Current Biology* 10, 919-S2.
- Lieber, M.R. (2010). The Mechanism of Double-Strand DNA Break Repair by the Nonhomologous DNA End-Joining Pathway. *Annu. Rev. Biochem.* 79, 181-211.
- Long, D.T., *et al.* (2014). BRCA1 Promotes Unloading of the CMG Helicase from a Stalled DNA Replication Fork. *Mol. Cell*.
- Long, D.T., *et al.* (2011). Mechanism of RAD51-dependent DNA interstrand cross-link repair. *Science* 333, 84-7.
- Lu, K., *et al.* (2010). Structural characterization of formaldehyde-induced cross-links between amino acids and deoxynucleosides and their oligomers. *Journal of the American Chemical Society* 132, 3388-99.
- Luria, S.E., and Delbrück, M. (1943). MUTATIONS OF BACTERIA FROM VIRUS SENSITIVITY TO VIRUS RESISTANCE. *Genetics* 28, 491-511.
- Lynch, H.T., *et al.* (2009). Review of the Lynch syndrome: history, molecular genetics, screening, differential diagnosis, and medicolegal ramifications. *Clinical genetics* 76, 1-18.
- Ma, T.-H., and Harris, M.M. (1988). Review of the genotoxicity of formaldehyde. *Mutation Research/Reviews in Genetic Toxicology* 196, 37-59.
- Machida, Y., *et al.* (2012). Spartan/C1orf124 is important to prevent UV-induced mutagenesis. *Cell cycle (Georgetown, Tex.)* 11, 3395-402.

Malik, M., and Nitiss, J.L. (2004). DNA repair functions that control sensitivity to topoisomerase-targeting drugs. *Eukaryotic cell* 3, 82-90.

Mao, Y., *et al.* (2000). SUMO-1 conjugation to topoisomerase I: A possible repair response to topoisomerase-mediated DNA damage. *Proceedings of the National Academy of Sciences of the United States of America* 97, 4046-51.

Mehta, A., and Haber, J.E. (2014). Sources of DNA Double-Strand Breaks and Models of Recombinational DNA Repair. *Cold Spring Harb Perspect Biol* 6.

Memisoglu, A., and Samson, L. (2000). Base excision repair in yeast and mammals. *Mutat. Res.* 451, 39-51.

Meyn, R.E., *et al.* (1987). The induction of DNA-protein crosslinks in hypoxic cells and their possible contribution to cell lethality. *Radiation research* 109, 419-29.

Mieczkowski, P.A., *et al.* (2006). Recombination between retrotransposons as a source of chromosome rearrangements in the yeast *Saccharomyces cerevisiae*. *DNA repair* 5, 1010-20.

Min, J.-H., and Pavletich, N.P. (2007). Recognition of DNA damage by the Rad4 nucleotide excision repair protein. *Nature* 449, 570-575.

Moldovan, G.L., and D'Andrea, A.D. (2009). How the fanconi anemia pathway guards the genome. *Annu. Rev. Genet.* 43, 223-49.

Moldovan, G.L., *et al.* (2007). PCNA, the maestro of the replication fork. *Cell* 129, 665-79.

Mosbech, A., *et al.* (2012). DVC1 (C1orf124) is a DNA damage-targeting p97 adaptor that promotes ubiquitin-dependent responses to replication blocks. *Nat. Struct. Mol. Biol.* 19, 1084-92.

Mullen, J.R., *et al.* (2010). Wss1 is a SUMO-dependent isopeptidase that interacts genetically with the Slx5-Slx8 SUMO-targeted ubiquitin ligase. *Mol. Cell. Biol.* 30, 3737-48.

Mullen, J.R., *et al.* (2011). Genetic evidence that polysumoylation bypasses the need for a SUMO-targeted Ub ligase. *Genetics* 187, 73-87.

Mumberg, D., *et al.* (1995). Yeast vectors for the controlled expression of heterologous proteins in different genetic backgrounds. *Gene* 156, 119-22.

Nakano, T., *et al.* (2003). DNA-protein cross-link formation mediated by oxanine. A novel genotoxic mechanism of nitric oxide-induced DNA damage. *J. Biol. Chem.* 278, 25264-72.

Noll, D.M., *et al.* (2006). Formation and repair of interstrand cross-links in DNA. *Chemical reviews* 106, 277-301.

Nouspikel, T. (2009). DNA repair in mammalian cells : Nucleotide excision repair: variations on versatility. *Cell. Mol. Life Sci.* 66, 994-1009.

- Ogi, T., *et al.* (2010). Three DNA polymerases, recruited by different mechanisms, carry out NER repair synthesis in human cells. *Molecular cell* *37*, 714-727.
- Pavlov, Y.I., *et al.* (2003). Evidence for preferential mismatch repair of lagging strand DNA replication errors in yeast. *Current biology* *13*, 744-748.
- Peak, M.J., *et al.* (1985). DIFFERENT (DIRECT and INDIRECT) MECHANISMS FOR THE INDUCTION OF DNA-PROTEIN CROSSLINKS IN HUMAN CELLS BY FAR- and NEAR-ULTRAVIOLET RADIATIONS (290 and 405 nm). *Photochemistry and Photobiology* *42*, 141-146.
- Pfander, B., *et al.* (2005). SUMO-modified PCNA recruits Srs2 to prevent recombination during S phase. *Nature* *436*, 428-33.
- Pommier, Y. (2006). Topoisomerase I inhibitors: camptothecins and beyond. *Nat Rev Cancer* *6*, 789-802.
- Pommier, Y., *et al.* (2006). Repair of Topoisomerase I - Mediated DNA Damage. In *Progress in Nucleic Acid Research and Molecular Biology*, M. Kivie, ed. (Academic Press), pp. 179-229.
- Pouliot, J.J., *et al.* (1999). Yeast gene for a Tyr-DNA phosphodiesterase that repairs topoisomerase I complexes. *Science* *286*, 552-5.
- Pourquier, P., *et al.* (1997). Effects of uracil incorporation, DNA mismatches, and abasic sites on cleavage and religation activities of mammalian topoisomerase I. *J. Biol. Chem.* *272*, 7792-6.
- Prasad, R., *et al.* (2000). FEN1 stimulation of DNA polymerase β mediates an excision step in mammalian long patch base excision repair. *Journal of Biological Chemistry* *275*, 4460-4466.
- Psakhye, I., and Jentsch, S. (2012). Protein Group Modification and Synergy in the SUMO Pathway as Exemplified in DNA Repair. *Cell* *151*, 807-820.
- Raschle, M., *et al.* (2008). Mechanism of replication-coupled DNA interstrand crosslink repair. *Cell* *134*, 969-80.
- Ravanat, J.-L., *et al.* (2014). Radiation-mediated formation of complex damage to DNA: a chemical aspect overview. *The British Journal of Radiology* *87*, 20130715.
- Regairaz, M., *et al.* (2011). Mus81-mediated DNA cleavage resolves replication forks stalled by topoisomerase I-DNA complexes. *J. Cell Biol.* *195*, 739-49.
- Renkawitz, J., *et al.* (2014). Mechanisms and principles of homology search during recombination. *Nat. Rev. Mol. Cell. Biol.* *15*, 369-83.
- Renkawitz, J., *et al.* (2013). Monitoring homology search during DNA double-strand break repair in vivo. *Mol. Cell* *50*, 261-72.
- Rosado, I.V., *et al.* (2011). Formaldehyde catabolism is essential in cells deficient for the Fanconi anemia DNA-repair pathway. *Nat. Struct. Mol. Biol.* *18*, 1432-4.

- Sale, J.E. (2013). Translesion DNA Synthesis and Mutagenesis in Eukaryotes. Cold Spring Harb. Perspect. Biol. 5.
- Sambrook, J. (2001). Molecular cloning : a laboratory manual, D.W. Russell, ed. (Cold Spring Harbor, N.Y. :: Cold Spring Harbor Laboratory Press).
- Sarbajna, S., and West, S.C. (2014). Holliday junction processing enzymes as guardians of genome stability. Trends Biochem. Sci. 39, 409-419.
- Schärer, O.D. (2013). Nucleotide Excision Repair in Eukaryotes. Cold Spring Harb. Perspect. Biol. 5.
- Sobol, R.W., *et al.* (1996). Requirement of mammalian DNA polymerase- β in base-excision repair. Nature 379, 183-186.
- Stapf, C., *et al.* (2011). The general definition of the p97/valosin-containing protein (VCP)-interacting motif (VIM) delineates a new family of p97 cofactors. J. Biol. Chem. 286, 38670-8.
- Stolz, A., *et al.* (2011). Cdc48: a power machine in protein degradation. Trends Biochem. Sci. 36, 515-23.
- Stucki, M., *et al.* (1998). Mammalian base excision repair by DNA polymerases delta and epsilon. Oncogene 17, 835-843.
- Su, D., and Hochstrasser, M. (2010). A WLM protein with SUMO-directed protease activity. Mol. Cell. Biol. 30, 3734-6.
- Subramanian, D., *et al.* (2001). ICE Bioassay. In DNA Topoisomerase Protocols, N. Osheroff, and M.-A. Bjornsti, eds. (Humana Press), pp. 137-147.
- Swenberg, J.A., *et al.* (2011). Endogenous versus exogenous DNA adducts: their role in carcinogenesis, epidemiology, and risk assessment. Toxicol. Sci. 120 Suppl 1, S130-45.
- Symington, L.S. (2014). End Resection at Double-Strand Breaks: Mechanism and Regulation. Cold Spring Harb Perspect Biol 6.
- Tishkoff, D.X., *et al.* (1998). Identification of a human gene encoding a homologue of *Saccharomyces cerevisiae* EXO1, an exonuclease implicated in mismatch repair and recombination. Cancer research 58, 5027-5031.
- Tsabar, M., and Haber, J.E. (2013). Chromatin modifications and chromatin remodeling during DNA repair in budding yeast. Current Opinion in Genetics & Development 23, 166-173.
- Ulrich, H.D., and Jentsch, S. (2000). Two RING finger proteins mediate cooperation between ubiquitin-conjugating enzymes in DNA repair. EMBO J 19, 3388-97.
- Vance, J.R., and Wilson, T.E. (2002). Yeast Tdp1 and Rad1-Rad10 function as redundant pathways for repairing Top1 replicative damage. Proceedings of the National Academy of Sciences of the United States of America 99, 13669-74.

Vare, D., *et al.* (2012). DNA interstrand crosslinks induce a potent replication block followed by formation and repair of double strand breaks in intact mammalian cells. *DNA repair* 11, 976-85.

Vermeulen, W., and Fousteri, M. (2013). Mammalian Transcription-Coupled Excision Repair. *Cold Spring Harb. Perspect. Biol.* 5.

West, R.B., *et al.* (1998). Productive and nonproductive complexes of Ku and DNA-dependent protein kinase at DNA termini. *Mol. Cell. Biol.* 18, 5908-20.

Wood, R.D. (1999). DNA damage recognition during nucleotide excision repair in mammalian cells. *Biochimie* 81, 39-44.

Zamble, D.B., and Lippard, S.J. (1995). Cisplatin and DNA repair in cancer chemotherapy. *Trends in Biochemical Sciences* 20, 435-439.

Zhang, H., *et al.* (1995). Radiation-induced DNA damage in tumors and normal tissues. III. Oxygen dependence of the formation of strand breaks and DNA-protein crosslinks. *Radiation research* 142, 163-8.

Zhang, J., and Walter, J.C. (2014). Mechanism and regulation of incisions during DNA interstrand cross-link repair. *DNA repair* 19, 135-142.

Zharkov, D.O. (2008). Base excision DNA repair. *Cell. Mol. Life Sci.* 65, 1544-65.

Abbreviations

5'-FOA	5-Fluoroorotic acid
A	Alanine
aa	Amino acid
ADH	Alcohol dehydrogenase
AFU	Arbitrary fluorescence units
ALDH	Acetaldehyde dehydrogenase
AP	Apurinic/apyrimidinic site
AU	Absorbance units
BER	Base Excision repair
BIR	Break induced replication
BLAST	Basic local alignment search tool
BLM	Bloom's helicase
bp	Base pair
BSA	Bovine serum albumin
cd	Catalytic domain
Chr	Chromosome
CPT	Camptothecin
Da	Dalton
DMSO	Dimethyl sulfoxide
DNA	Deoxyribonucleic acid
DPC	DNA-protein crosslink
DSB	Double-strand break
E	Glutamate
EDTA	Ethylenediaminetetraacetic acid
EMSA	Electrophoretic mobility shift assay
Exo1	Exonuclease 1
FA	Formaldehyde
FANCD	Fanconi anemia proteins
g	Gram
G1-phase	Gap 1 phase
G2-phase	Gap 2 phase
GCR	Gross chromosomal rearrangements
GGR	Global genome repair
GST	Glutathione S-transferase
H	Histidine
H1	Histone H1
HA	Human influenza hemagglutinin
Hmg1	High mobility group 1
HNPCC	hereditary nonpolyposis colon cancer
HR	Homologous recombination
hr(s)	Hour(s)
ICL	Inter-strand crosslink
IR	Ionizing radiation
M	Molar

min	Minute
MMR	Mismatch repair
NER	Nucleotide excision repair
NHEJ	Non-homologous end joining
NO	Nitric oxide
OD	Optical density
PAGE	Polyacrylamide gel electrophoresis
PBS	Phosphate buffered saline
PCNA	Proliferating cell nuclear antigen
PCR	Polymerase chain reaction
PIP	PCNA interacting protein
PRR	Postreplicative repair
Q	Glutamine
RFU	Relative fluorescence units
RNS	Reactive nitrogen species
ROS	Reactive oxygen species
RPA	Replication protein A
RT	Room temperature
S-phase	Synthesis phase
<i>S. cerevisiae</i>	<i>Saccharomyces cerevisiae</i>
<i>S. pombe</i>	<i>Schizosaccharomyces pombe</i>
SC	Synthetic complete
SDS	Sodium dodecyl sulfate
SGA	Synthetic gene array
SIM	SUMO interacting motif
SSB	Single-strand break
TCA	Trichloroacetic acid
TCR	Transcripton coupled repair
Tdp1	Tyrosyl-DNA phosphodiesterase 1
TLS	Translesion synthesis
Top1	Topoisomerase 1
Top1cc	Top1 cleavage complex
Top2	Topoisomerase 2
Ubi	Ubiquitin
UBL	Ubiquitin-like
UBZ	Ubiquitin binding zinc finger
UV	Ultraviolet
VIM	VCP interacting motif
WCE	Whole cell extract
Wss1	Weak suppressor of smt3
WT	Wildtype
XP	Xeroderma pigmentosum
YPD	Yeast extract peptone dextrose
β-ME	β-mercaptoethanol

Acknowledgements

I would like to thank my PhD supervisor Stefan Jentsch for his great advice and support in all matters, work-related and personal. Stefan, I am really grateful for the interesting and insightful discussions, the freedom you provide, your ambition and the great atmosphere in your lab.

Moreover, I would like to thank the members of the thesis committee for kindly agreeing to referee this thesis. I am especially thankful to Peter Becker not only for co-refereeing this thesis, but also for his career advice and support.

I am also deeply thankful for Alex's excellent technical support and his extraordinary dedication. His support was instrumental for the success of this study. Many thanks also go to Jochen for his help in setting up the robot-based assays and his assistance with all IT-related matters. In addition, I would like to thank Massimo for providing endless amounts of agar plates, which were essential for this study. Furthermore, I would like to thank the MPI's core facility, especially Claudia and Sabine, for the never-ending supply of recombinant Wss1.

Many thanks go to Peter and Nico. I always enjoyed our common time in the lab very much; it was really fantastic to collaborate with you guys. Of course, I would also like to express my sincere gratitude to all members of the department, especially highlighting Boris, Claudio, Florian P., Florian W., Frank, Irina, Jörg, Kefeng, Markus, Max, Ramazan, Sean, Sittinan and Steven. Thank you for the good times in the lab and all the interesting discussions.

A great and warm thank you goes to my family, who was always extremely supportive during my entire life. Finally, from the bottom of my heart I would like to thank my own small family, Silvia and Tom, for the love and joy they bring into my life; and especially Silvia for her perpetual understanding and support.

Curriculum Vitae - Julian Stingele

Academic Education

since 04/2010	PhD studies Supervisor: Prof. Dr. S. Jentsch, MPI of Biochemistry, Martinsried
03/2010	Diploma thesis Supervisor: Dr. S. Raasi, University of Konstanz
10/2007 - 06/2009	University of Konstanz, Germany
06/2003	High school diploma: Württemberg-Gymnasium, Stuttgart

Publications

Stingele, J., Habermann, B. and Jentsch, S.
DNA-protein crosslink repair: proteases as DNA repair enzymes.
Trends Biochem. Sci., commissioned review in preparation.

Stingele, J., Schwarz, M.S., Bloemeke, N., Wolf, P.G. and Jentsch, S. (2014)
A DNA-dependent protease involved in DNA-protein crosslink repair.
Cell, 158:327-38.

Stingele, J., Roder, U.W. and Raasi, S. (2012)
Surface plasmon resonance to measure interactions of UbFs with their binding partners.
Methods Mol. Biol., 832, 263-77.

Hänzelmann, P.*, **Stingele, J.***, Hofmann, K., Schindelin, H. and Raasi, S. (2010)
The yeast E4 ubiquitin ligase Ufd2 interacts with the ubiquitin-like domains of Rad23 and Dsk2 via a novel and distinct ubiquitin-like binding domain.
J. Biol. Chem., 285, 20390-8.
***equal contribution**

Awards and Honors

Max Planck Institute of Biochemistry Junior Research Award 2014

Selected to participate as 'young researcher' at the 64th Lindau Nobel Laureate Meeting, Lindau, Germany (June 29 - July 4, 2014)